INTERNATIONAL JOURNAL FOR NUMERICAL METHODS IN ENGINEERING

Int. J. Numer. Meth. Engng 2000; **00**:1–6 *Prepared using* nmeauth.cls *[Version: 2002/09/18 v2.02]*

An energy momentum conserving algorithm using the variational formulation of visco-plastic updates

L. Noels[†], L. Stainier[‡*], J.-P. Ponthot

University of Liège, LTAS-Milieux Continus & Thermomécanique, Chemin des Chevreuils 1, B-4000 Liège, Belgium

SUMMARY

In this paper we use the variational formulation of elasto-plastic updates proposed by Ortiz and Stainier [*Computer Methods in Applied Mechanics and Engineering*, 1999] in the context of consistent time integration schemes. We show that such a formulation is well suited to obtain a general expression of energy momentum conserving algorithms. Moreover, we present numerical examples that illustrate the efficiency of our developments. Copyright © 2000 John Wiley & Sons, Ltd.

KEY WORDS: Energy conserving; momentum conserving; dynamics; variational formulation; elasto-plasticity; finite-elements method

*Correspondence to: L. Stainier, Tel: +32-(0)4-366-9152, Fax: +32-(0)4-366-9141, E-mail: l.stainier@ulg.ac.be

[†]Research Fellow at the Belgian National Fund for Scientific Research (FNRS)

[‡]Research Associate at the Belgian National Fund for Scientific Research (FNRS)

Received

Revised

1. INTRODUCTION

One can resort to two families of algorithms to integrate the equations of evolution of dynamical systems: the implicit family and the explicit family. In this paper, we focus on the implicit family. The most widely used implicit algorithm is the Newmark algorithm [1]. For linear models, this algorithm is unconditionally stable. For non-linear models, Belytschko and Schoeberle [2] proved that the discrete energy, computed from the work of internal forces and from the kinetic energy, is bounded if it remains positive. Nevertheless, since the work of internal forces is different from the internal energy variation when the Newmark algorithm is used in the non-linear range, Hughes et al. [3] have proved that Newmark algorithm remains physically consistent only for small time step sizes. To avoid divergence due to numerical instabilities, numerical damping was thus introduced, leading to the generalized-α methods [4]. Nevertheless, the unconditional stability of these methods is guaranteed only for linear systems or asymptotically for the high frequencies in the non-linear range [5].

To overcome that drawback, a new class of algorithms, verifying the conservation laws in the non-linear range, appeared. To demonstrate stability, these new algorithms were not studied on a linear system as the previous ones, but were studied by taking into account non-linearities. The first algorithm verifying these properties was proposed by Simo and Tarnow [6]. They called this algorithm "Energy Momentum Conserving Algorithms" or EMCA. It consists in a mid-point scheme with an adequate evaluation of the internal forces. This adequate evaluation was given for a Saint Venant-Kirchhoff hyperelastic material. A generalization to other hyperelastic models was given by Laursen and Meng [7], who iteratively solve a new equation for each Gauss point to determine the adequate second Piola-Kirchhoff stress tensor. Another solution that avoids this iterative procedure leads to a general formulation in term of

the second Piola-Kirchhoff stress tensor, as proposed by Gonzalez [8]. This formulation is valid for general hyperelastic materials. The EMCA was then extended to dynamic finite deformation plasticity based on a hyperelastic model by Meng and Laursen [9, 10], and to dynamic finite deformation plasticity based on a hypoelastic model by the present authors [11, 12]. In such formulations, the algorithm remains energy conserving when no plastic deformation occurs, and "dissipates energy in a manner consistent with the physical model in use" (sic [9]) when plastic deformation occurs. Recently, contrarily to Gonzalez [8] who proposed a particular expression of the second Piola-Kirchhoff stress tensor to reach the conserving properties, Sansour *et al.* [13] have proposed an expression (restrained to elasticity) by integrating the second Piola-Kirchhoff stress tensor in time. The expression thus obtained is therefore less arbitrary than that of Gonzalez.

In the same context, for contact treatment, a penalty method was developed to simulate non-frictional and frictional contact interactions by Armero and Petöcz [14, 15]. This method allows surface penetration but ensures conservation of the energy for frictionless problems and consistent dissipation for frictional ones. Laursen and Chawla [16, 17] developed Lagrangian and augmented Lagrangian methods to simulate non-frictional and frictional contact. Finally to avoid the lack of convergence due to the presence of high frequency modes, numerical dissipation was introduced in the conserving algorithms by Armero and Romero [18, 19] for hyperelastic materials. In the same way, Noels *et al.* [20] introduced dissipation for hypoelastic materials.

Let us note that the properties of conservation can be reached by using a Petrov-Galerkin time finite-element method as described by Betsch and Steinmann [21, 22]. They can also be satisfied by using an approximation of the time Galerkin method as proposed by Bauchau and

Joo [23]. In the same way, an approximation of the time discontinuous Galerkin method leads to an Energy Decaying scheme [23] that presents some numerical dissipation. Another Energy Preserving/Decaying algorithm can also be obtained using a Runge-Kutta method (*e.g.* [24]).

Let us now focus on the plasticity treatments leading to an energy-momentum conserving scheme. The hyperelastic-based formulation, proposed by Meng and Laursen [9, 10] is based on the elastic formulation proposed by Gonzalez [8] and is restrained to isotropic hardening. The hypoelastic-based formulation, as proposed by Noels *et al.* [11, 12], can additionally account for kinematic hardening but suffers from other restrictions (Hooke's parameter needs to be constant and no internal potential can be defined). In this paper we propose a more general hyperelastic-based formulation, using the variational visco-plastic constitutive updates proposed by Ortiz and Stainier [25]. The mathematical structure of this formulation provides many interesting features, e.g. for error estimation [26]. The main feature of this formulation is that the stress tensor always derives from an incremental potential, even if plastic deformations occur. Therefore, in such a framework we can use the formulation based on the second Piola-Kirchhoff stress tensor as proposed by Gonzalez [8] without any modification. Moreover, the use of the variational formulation does not lead to any *a priori* restrictions on the material laws or parameters, even if in this paper we focus on elasto-plasticity with isotropic hardening. Finally, we think that the use of the variational updates can be compatible with the method proposed by Sansour *et al.* [13], even if in this paper we focus on the method proposed by Gonzalez [8].

The plan of the paper is the following. Section 2 will expose preliminaries such as the dynamic conservation laws and the finite-element discretization. We will also explain the split of the internal potential leading to a locking-free element. In section 3, we will recall the variational

formulation of elasto-plasic updates. In section 4, we will use this formulation in combination with the Gonzalez method to design an energy-momentum conserving scheme. In section 5 we will show the accuracy and consistency of the proposed algorithm on numerical examples. Finally we will draw some conclusions.

2. PRELIMINARIES

In this section we will define the notations in use in this work. Therefore we will be able to recall the continuum laws. Then we will introduce the finite-element discretization. In this work we will use a quasi-incompressible formulation.

2.1. Notations

Let $\mathbb{V} \subset \mathbb{R}^3$ be the manifold of points defining the body and $\mathbb{S} \subset \mathbb{R}^3$ be the manifold of its boundary. Since we will work with regular bodies in Euclidean space, we will identify the body with the space it occupies and will freely pass between the material and spatial descriptions of a field whenever it is convenient to do so. We define two configurations: the initial configuration referred to by subscript 0 and the current configuration at time t. Let ρ_0: $\mathbb{V}_0 \rightarrow \mathbb{R}_+$ be the initial density. Boundary $\mathbb{S}$ is decomposed into two parts: the first one $\mathbb{S}_{\vec{x}}$ is the part where the displacements are known and the second one $\mathbb{S}_{\vec{T}}$ is the part where the surface tractions are known. It yields $\mathbb{S}_{\vec{x}} \cup \mathbb{S}_{\vec{T}} = \mathbb{S}$ and $\mathbb{S}_{\vec{x}} \cap \mathbb{S}_{\vec{T}} = 0$. Let us note that in case of interaction between different bodies this theory has to be rewritten to take into account the contact forces between different bodies, but it does not modify results we use to describe body deformations. Let $\vec{x}$ be the current positions and $\vec{x}_0$ be the initial positions. Therefore, the two-point gradient of

deformation tensor is defined by

$$\mathbf{F} \equiv \frac{\partial \vec{x}}{\partial \vec{x}_0} \quad \text{with} \quad \mathbf{f} \equiv \mathbf{F}^{-1} \text{ and } J \equiv \det\mathbf{F} \tag{1}$$

The right Cauchy-Green strain tensor is defined by

$$\mathbf{C} \equiv \mathbf{F}^T\mathbf{F} \tag{2}$$

Conservation of the mass leads to

$$\rho d\mathbb{V} = \rho_0 d\mathbb{V}_0 \quad \text{and} \quad \rho J = J_0 \tag{3}$$

To use the quasi-incompressible technique as proposed by Simo and Taylor [27] we need more definitions. Let θ^e (physical meaning of θ^e will be deduced later) be a constant scalar on the volume part $\mathbb{V}_0^e$, with $\bigcup_e \mathbb{V}_0^e = \mathbb{V}_0$ and $\bigcap_e \mathbb{V}_0^e = 0$. Exponent e will refer to values for the volume part $\mathbb{V}_0^e$ (for a finite-element decomposition, e will be the index of an element). Let the two modified gradients of deformation $\hat{\mathbf{F}}$ and $\bar{\mathbf{F}}$, the first one having unitary determinant, defined by

$$\hat{\mathbf{F}} \equiv J^{-\frac{1}{3}}\mathbf{F} \quad \text{and} \quad \bar{\mathbf{F}} \equiv \theta^{e\,\frac{1}{3}}\hat{\mathbf{F}} = \left[\frac{\theta^e}{J}\right]^{\frac{1}{3}}\mathbf{F} \tag{4}$$

In the same way, the two modified right Cauchy-Green strain tensors are defined by

$$\hat{\mathbf{C}} \equiv \hat{\mathbf{F}}^T\hat{\mathbf{F}} = \left[\frac{1}{J}\right]^{\frac{2}{3}}\mathbf{C} \quad \text{and} \quad \bar{\mathbf{C}} \equiv \bar{\mathbf{F}}^T\bar{\mathbf{F}} = \left[\frac{\theta^e}{J}\right]^{\frac{2}{3}}\mathbf{C} \tag{5}$$

Let $\mathbb{X}$ be the manifold of admissible positions

$$\mathbb{X} \equiv \left\{\vec{x} : \mathbb{V}_0 \to \mathbb{R}^3 \middle| \left[J > 0 \text{ and } \vec{x}|_{\mathbb{S}_{\vec{x}}} = \bar{\vec{x}}\right] \ \forall \vec{x}_0 \in \mathbb{V}_0\right\} \tag{6}$$

with $\bar{\vec{x}}$ the known (imposed) positions. Let t be the current time and let $\mathbb{T} = [0, t_f]$ be the time integration interval. Therefore, the motion of the body is defined by $t \in \mathbb{T} \to \vec{x}(t) \in \mathbb{X}$. During this motion, the body is subject to specific loads $\vec{b}(t) : \mathbb{V}_0 \times \mathbb{T} \to \mathbb{R}^3$. Let $\boldsymbol{\Sigma}$ be the Cauchy stress

tensor. Boundary pressures $\vec{T}_S(t) : \mathbb{S}_{\vec{T}_0} \times \mathbb{T} \to \mathbb{R}^3$ verify the condition $\vec{T}_S(t) = \mathbf{\Sigma}(t)\,\vec{n}(t)$ with $\vec{n}$ the outward unit normal to $\mathbb{S}$.

When the body is decomposed into finite elements thanks to shape functions φ^ξ: $\mathbb{V}_0 \to \mathbb{R}$ with $\xi \in [1, N]$ (N the total number of nodes), and with $\varphi^\xi(\vec{x}_0^{\,\mu}) = \delta_\xi^\mu$ (δ is the Kronecker symbol), it leads for each node $\xi \in [1, N]$

$$\vec{x}(\vec{x}_0) = \varphi^\xi(\vec{x}_0)\,\vec{x}^\xi \quad , \dot{\vec{x}}(\vec{x}_0) = \varphi^\xi(\vec{x}_0)\,\dot{\vec{x}}^\xi \text{ and } \ddot{\vec{x}}(\vec{x}_0) = \varphi^\xi(\vec{x}_0)\,\ddot{\vec{x}}^\xi \tag{7}$$

where Einstein's notations have been used. Let $\vec{v}$ be an admissible virtual displacement defined by the manifold

$$\mathbb{D} \equiv \left\{\vec{v} : \mathbb{V}_0 \to \mathbb{R}^3 \middle| \left[\vec{v}|_{\mathbb{S}_{\vec{x}}} = 0 \text{ et } \vec{v}(\vec{x}_0, 0) = 0, \vec{v}(\vec{x}_0, t_f) = 0\ \forall \vec{x}_0 \in \mathbb{V}_0\right]\right\} \tag{8}$$

Let $\mathbb{D}^v \subset \mathbb{D}$ be the manifold of admissible virtual displacements $\delta\vec{x}$ that can be decomposed such as (7). In this manifold of test functions, we have introduced boundary conditions for the initial time and for the final time. These conditions are needed when using the principle of virtual work.

2.2. The continuous problem

The following quasi-variational principle (principle of virtual power of forces) must hold $\forall \delta\vec{x} \in \mathbb{D}^v$ [28, page 412]

$$\int_0^{t_f} \left\{ \int_{\mathbb{V}} \left[\rho \ddot{\vec{x}} \cdot \delta\vec{x} + \mathbf{\Sigma}^T : \frac{\partial \delta\vec{x}}{\partial \vec{x}} - \rho\vec{b} \cdot \delta\vec{x} \right] d\mathbb{V} - \int_{\mathbb{S}_{\vec{T}}} \left[\vec{T}_S \cdot \delta\vec{x} \right] d\mathbb{S} \right\} dt = 0 \tag{9}$$

where $\vec{a} \cdot \vec{b} = \vec{a}_i \vec{b}_i$ and where $\mathbf{A} : \mathbf{B} = \mathbf{A}_{ij}\mathbf{B}_{ij}$. Let $\mathbf{PK}$ be the second Piola-Kirchhoff stress tensor defined by

$$\mathbf{PK} = J\mathbf{F}^{-1}\mathbf{\Sigma}\mathbf{F}^{-T} \tag{10}$$

Using relation (3) and (10), integrating (9) by parts leads to

$$\underbrace{\int_{\mathbb{V}_0}\left\{\rho_0\ddot{\vec{x}}\cdot\delta\vec{x}\right\}d\mathbb{V}_0}_{\equiv\delta K} = \underbrace{\int_{\mathbb{V}_0}\left\{\rho_0\vec{b}\cdot\delta\vec{x}\right\}d\mathbb{V}_0+\int_{\mathbb{S}_{\vec{T}}}\left\{\vec{T}_S\cdot\delta\vec{x}\right\}d\mathbb{S}}_{\equiv\delta W_{\text{ext}}} - \underbrace{\int_{\mathbb{V}}\left\{\mathbf{FPK}^T:\frac{\partial\delta\vec{x}}{\partial\vec{x}_0}\right\}d\mathbb{V}_0}_{\equiv\delta W_{\text{int}}} \quad \forall t\in\mathbb{T} \tag{11}$$

where δW_{int}, δW_{ext} and δK are respectively the virtual work of internal forces, the virtual work of external forces and the virtual work of inertia forces. This principle leads to the dynamics conservation laws.

2.2.1. Conservation of linear momentum. Let $\vec{L}$ be the linear momentum defined by

$$\vec{L} \equiv \int_{\mathbb{V}_0}\left\{\rho_0\dot{\vec{x}}\right\}d\mathbb{V}_0 \tag{12}$$

where relation (3) has been used. Assuming pure Neumann boundary conditions (*i.e.* $\mathbb{S}_{\vec{x}}=\emptyset$), if $\delta\vec{x}\in\mathbb{D}^v$ is taken constant, relation (11) leads to the conservation of the linear momentum

$$\dot{\vec{L}} = \underbrace{\int_{\mathbb{V}_0}\left\{\rho_0\vec{b}\right\}d\mathbb{V}+\int_{\mathbb{S}_{\vec{T}}}\left\{\vec{T}_S\right\}d\mathbb{S}}_{\equiv\vec{F}_{\text{ext}}} \quad \forall t\in\mathbb{T} \tag{13}$$

2.2.2. Conservation of angular momentum. Let $\vec{J}$ be the angular momentum defined by

$$\vec{J} \equiv \int_{\mathbb{V}_0}\left\{\rho_0\vec{x}\wedge\dot{\vec{x}}\right\}d\mathbb{V}_0 \tag{14}$$

Assuming pure Neumann boundary conditions (*i.e.* $\mathbb{S}_{\vec{x}}=\emptyset$), taking $\delta\vec{x}=\vec{\eta}\wedge\vec{x}$ with $\vec{\eta}$ constant, since **PK** is symmetric, and $\vec{\eta}$ is an arbitrary constant, relation (11) leads to the conservation of the angular momentum

$$\dot{\vec{J}} = \int_{\mathbb{V}_0}\left\{\rho_0\vec{x}\wedge\vec{b}\right\}d\mathbb{V}_0+\int_{\mathbb{S}_{\vec{T}}}\left\{\vec{x}\wedge\vec{T}_S\right\}d\mathbb{S} \quad \forall t\in\mathbb{T} \tag{15}$$

2.2.3. Conservation of the energy. Let K, $W_{\rm int}$ and $W_{\rm ext}$ respectively be the kinetic energy, the internal forces power and the external forces power, with

$$\begin{aligned} K &\equiv \int_{\mathbb{V}_0} \left\{ \frac{1}{2}\rho_0 \dot{\vec{x}}^2 \right\} d\mathbb{V}_0 \\ \dot{W}_{\rm int} &\equiv \int_{\mathbb{V}_0} \left\{ \mathbf{P}\mathbf{K}^T : \left[\mathbf{F}^T \dot{\mathbf{F}} \right] \right\} d\mathbb{V}_0 \\ \dot{W}_{\rm ext} &\equiv \int_{\mathbb{V}_0} \left\{ \rho_0 \vec{b} \cdot \dot{\vec{x}} \right\} d\mathbb{V}_0 + \int_{\mathbb{S}_{\vec{T}}} \left\{ \vec{T}_S \cdot \dot{\vec{x}} \right\} d\mathbb{S} \end{aligned} \tag{16}$$

where relation (3) has been used. If the power of internal forces $\dot{W}_{\rm int}$ is decomposed into a reversible part $\dot{W}^{\rm el}_{\rm int}$ and an irreversible part $\dot{W}^{\rm pl}_{\rm int} \geq 0$ (plastic dissipation, ...) and if E is the system energy, one gets

$$\dot{W}_{\rm int} \equiv \dot{W}^{\rm el}_{\rm int} + \dot{W}^{\rm pl}_{\rm int} \quad \text{and} \quad E \equiv K + W^{\rm el} \tag{17}$$

Therefore, assuming pure Neumann boundary conditions (*i.e.* $\mathbb{S}_{\vec{x}} = \emptyset$), if $\delta\vec{x} = \dot{\vec{x}}$, relation (11) leads to the first thermodynamics principle

$$\dot{E} = \dot{W}_{\rm ext} - \dot{W}^{\rm pl}_{\rm int} \quad \forall t \in \mathbb{T} \tag{18}$$

Let us assume that, even when internal dissipation occurs, we can write

$$\mathbf{P}\mathbf{K} = 2\frac{\partial D_{\rm eff}}{\partial \mathbf{C}} \tag{19}$$

with $\mathbf{C}$ defined by relation (2), and with $D_{\rm eff}$ the effective stress potential. Therefore, using the symmetry of the stress tensor $\mathbf{PK}$, $\dot{W}_{\rm int}$ defined in relation (16) can be rewritten as

$$\dot{W}_{\rm int} = \int_{\mathbb{V}_0} \left\{ \dot{D}_{\rm eff} \right\} d\mathbb{V}_0 \tag{20}$$

and relations (17) and (18) are rewritten as

$$\dot{K} + \int_{\mathbb{V}_0} \left\{ \dot{D}_{\rm eff} \right\} d\mathbb{V}_0 = \dot{W}_{\rm ext} \quad \forall t \in \mathbb{T} \tag{21}$$

Nevertheless, a direct application of the finite element method to expression (20) can lead to pressure-locking problems in the case of (quasi-)incompressible behaviors such as those encountered in viscoplasticity. To overcome this, we use the modification proposed by Simo and Taylor [27]. It is important to note that for materials without incompressibility constraints, one could directly proceed with a standard finite element discretization of the problem, without loosing any of the consistency properties. Our formalism can easily be simplified for this approach.

2.2.4. Quasi-incompressible technique. Using relations (4) and (5), with θ^e a constant value on the volume part $\mathbb{V}_0^e$, the internal energy on the volume part $\mathbb{V}_0^e$ can be rewritten as a modified internal energy $\bar{W}_{\text{int}}^e\left(\vec{x}_0, \bar{\mathbf{C}}\left(\vec{x}, \theta^e\right)\right)$ depending on θ^e and depending on the positions $\vec{x}$. Let p^e be constant for each volume part $\mathbb{V}_0^e$ (physical meaning of p^e will be deduced later). Then Simo and Taylor [27] proposed, for each volume part $\mathbb{V}_0^e$, the following expression[†]

$$\delta W_{\text{int}}^e\left(\vec{x}, \theta^e, p^e\right) \equiv \delta \int_{\mathbb{V}_0^e} \left\{ D_{\text{eff}}\left(\vec{x}_0, \bar{\mathbf{C}}\left(\vec{x}, \theta^e\right)\right) + p^e\left[J - \theta^e\right] \right\} d\mathbb{V}_0^e \tag{22}$$

where $D_{\text{eff}}\left(\vec{x}_0, \bar{\mathbf{C}}\left(\vec{x}, \theta^e\right)\right)$ is the new effective internal energy which is a particular choice of $D_{\text{eff}}\left(\vec{x}_0, \vec{x}\right)$. Since neither δK, nor δW_{ext} depend on p^e, the variational principle, applied to p^e, leads to the definition of θ^e

$$\theta^e = \frac{1}{\mathbb{V}_0^e} \int_{\mathbb{V}_0^e} \{J\}\, d\mathbb{V}_0^e \tag{23}$$

that represents the mean volumic deformation of $\mathbb{V}_0^e$. In the same way, one has

$$p^e = \frac{1}{\mathbb{V}_0^e} \int_{\mathbb{V}_0^e} \left\{ \frac{\partial D_{\text{eff}}\left(\vec{x}_0, \bar{\mathbf{C}}\left(\vec{x}, \theta^e\right)\right)}{\partial \theta^e} \right\} d\mathbb{V}_0^e \tag{24}$$

[†]This expression is similar to the 3-field Hu-Washizu-Fraeijs de Veubeke (HWF) variational principle [29–31] (regarding denomination, see also [32]).

Finally, it yields

$$\frac{\partial W^e_{\text{int}}}{\partial \vec{x}} \cdot \delta\vec{x} = \int_{\mathbb{V}^e_0} \left\{ \frac{\partial D_{\text{eff}}\left(\vec{x}_0, \bar{\mathbf{C}}\left(\vec{x}, \theta^e\right)\right)}{\partial \vec{x}} \cdot \delta\vec{x} + p^e \frac{\partial J}{\partial \vec{x}} \cdot \delta\vec{x} \right\} d\mathbb{V}^e_0 \tag{25}$$

Since Gâteau derivatives lead to

$$\frac{\partial J}{\partial \vec{x}}\delta\vec{x} = J\text{tr}\frac{\partial \delta\vec{x}}{\partial \vec{x}} \quad \text{and} \quad \frac{\partial \bar{\mathbf{C}}}{\partial \vec{x}} \cdot \delta\vec{x} = 2\bar{\mathbf{F}}^T \frac{\partial \delta\vec{x}}{\partial \vec{x}}^T \bar{\mathbf{F}} - \frac{2}{3}\bar{\mathbf{C}}\text{tr}\frac{\partial \delta\vec{x}}{\partial \vec{x}} \tag{26}$$

relation (25) can be rewritten as

$$\frac{\partial W^e_{\text{int}}}{\partial \vec{x}} \cdot \delta\vec{x} = \int_{\mathbb{V}^e_0} \left\{ \left[2\text{dev}\left(\bar{\mathbf{F}} \frac{\partial D_{\text{eff}}}{\partial \bar{\mathbf{C}}} \bar{\mathbf{F}}^T \right) + p^e J\mathbf{I} \right] : \frac{\partial \delta\vec{x}}{\partial \vec{x}}^T \right\} d\mathbb{V}^e_0 \tag{27}$$

where $\text{dev}\mathbf{A}_{ij} \equiv \mathbf{A}_{ij} - \frac{1}{3}\text{tr}\mathbf{A}\delta_{ij}$ defines the deviatoric part of a tensor. Thanks to this relation it appears that p^e is the constant pressure associated to the volume $\mathbb{V}^e_0$

2.3. Finite-elements decomposition

Thanks to relation (7), the discrete variation of kinetic energy and of external energy from relation (11) can be rewritten as

$$\begin{aligned} \delta K &= \int_{\mathbb{V}_0} \left\{ \rho_0 \varphi^\xi \varphi^\mu \right\} d\mathbb{V}_0 \left[\ddot{\vec{x}} \right]^\mu \cdot \delta\vec{x}^\xi = M^{\xi\mu} \left[\ddot{\vec{x}} \right]^\mu \cdot \delta\vec{x}^\xi \\ \delta W_{\text{ext}} &= \int_{\mathbb{V}_0} \left\{ \rho_0 \vec{b} \varphi^\xi \right\} d\mathbb{V}_0 \cdot \delta\vec{x}^\xi + \int_{\mathbb{S}_{\vec{T}}} \left\{ \vec{T}_S \varphi^\xi \right\} d\mathbb{S} \cdot \delta\vec{x}^\xi = \left[\vec{F}_{\text{ext}} \right]^\xi \cdot \delta\vec{x}^\xi \end{aligned} \tag{28}$$

where $M^{\xi\mu}$ is the mass related to nodes ξ and μ. Using the quasi-incompressible method, the variation of the internal energy is defined from relation (27), where $\mathbb{V}^e_0$ represents a single finite-element. Therefore, using the following definition of the internal forces at node ξ

$$\vec{F}^\xi_{\text{int}} = \bigcup_e \int_{\mathbb{V}^e_0} \left\{ \left[2\text{dev}\left(\bar{\mathbf{F}} \frac{\partial D_{\text{eff}}}{\partial \bar{\mathbf{C}}} \bar{\mathbf{F}}^T \right) + p^e J\mathbf{I} \right] \mathbf{f}^T \vec{D}^\xi \right\} d\mathbb{V}^e_0 \tag{29}$$

where $\vec{D}^\xi \equiv \frac{\partial \varphi^\xi}{\partial \vec{x}_0}$ is the derivative, in the initial configuration, of the shape functions. Using relations (28) and since $\delta\vec{x} \in \mathbb{D}^v$ is an arbitrary vector, relations (11) and (27) lead to the

balance equation

$$M^{\xi\mu}\left[\ddot{\vec{x}}\right]^{\mu} = \left[\vec{F}_{\text{ext}} - \vec{F}_{\text{int}}\right]^{\xi} \quad \forall t \in \mathbb{T} \tag{30}$$

Let us note that internal forces (29) can be rewritten as

$$\vec{F}^{\xi}_{\text{int}} = \int_{\mathbb{V}^e_0} \left\{ \mathbf{F} \left[2 \left[\frac{\theta^e}{J}\right]^{\frac{2}{3}} \text{DEV}\frac{\partial D_{\text{eff}}}{\partial \bar{\mathbf{C}}} + p^e J \mathbf{C}^{-1} \right] \vec{D}^{\xi} \right\} d\mathbb{V}^e_0 \tag{31}$$

with $\text{DEV}\mathbf{A} \equiv \mathbf{A} - \frac{1}{3}\mathbf{A} : \mathbf{C}\mathbf{C}^{-1}$ the deviatoric operation in the reference configuration. Since

$$\frac{\partial \bar{\mathbf{C}}}{\partial \mathbf{C}} = \left[\frac{\theta^e}{J}\right]^{\frac{2}{3}} \left[\mathcal{I} - \frac{1}{3}\mathbf{C}\otimes\mathbf{C}^{-1}\right] \tag{32}$$

with $\mathcal{I}_{ijkl} = \frac{1}{2}\delta_{ik}\delta_{jl} + \frac{1}{2}\delta_{il}\delta_{jk}$ and $[\mathbf{A}\otimes\mathbf{B}]_{ijkl} = \mathbf{A}_{ij}\mathbf{B}_{kl}$, relation (31) can be rewritten as

$$\vec{F}^{\xi}_{\text{int}} = \int_{\mathbb{V}^e_0} \left\{ \mathbf{F} \underbrace{\left[2\frac{\partial D_{\text{eff}}}{\partial \mathbf{C}} + p^e J \mathbf{C}^{-1} \right]}_{\mathbf{PK}} \vec{D}^{\xi} \right\} d\mathbb{V}^e_0 \tag{33}$$

To be able to integrate the balance equation (30) in time, $\mathbb{T}$ is decomposed into some intervals $\left[t^n, t^{n+1}\right]$ such that $\mathbb{T} = \bigcup_{n=0}^{n=n^f} \left[t^n, t^{n+1}\right]$. Let $\Delta t = t^{n+1} - t^n$ be the time step size. Superscripts n and $n+1$ will refer to configurations at time t^n and t^{n+1}. To be consistent, the integration scheme must verify relations (13), (15) and (21).

Now we will explain how $\frac{\partial D_{\text{eff}}}{\partial \bar{\mathbf{C}}}$ and p^e can be computed.

2.3.1. Split of the internal potential. To simplify the above relations, let D_{eff} be split into a volumic part $\Phi^{\text{vol}}(\theta^e)$ (depending only on $\det\bar{\mathbf{F}} = \theta^e$ assumed constant for each element), and into a deviatoric part $\hat{D}_{\text{eff}}$, with

$$D_{\text{eff}}\left(\vec{x}_0, \bar{\mathbf{C}}(\vec{x}, \theta^e)\right) = \Phi^{\text{vol}}(\theta^e) + \hat{D}_{\text{eff}}\left(\hat{\mathbf{C}}\right) \tag{34}$$

Then relation (24) can directly be evaluated by

$$p^e = \frac{\partial \Phi^{\text{vol}}(\theta^e)}{\partial \theta^e} \tag{35}$$

Since

$$\frac{\partial \hat{\mathbf{C}}}{\partial \mathbf{C}} = \left[\frac{1}{J}\right]^{\frac{2}{3}} \left[\mathcal{I} - \frac{1}{3}\mathbf{C} \otimes \mathbf{C}^{-1}\right] \tag{36}$$

and since $\mathbf{C} \otimes \mathbf{C}^{-1} = \hat{\mathbf{C}} \otimes \hat{\mathbf{C}}^{-1}$, the deviatoric stress can be simplified into

$$2\frac{\partial D_{\text{eff}}}{\partial \mathbf{C}} = \left[\frac{1}{J}\right]^{\frac{2}{3}} 2\left[\frac{\partial \hat{D}_{\text{eff}}}{\partial \hat{\mathbf{C}}} - \frac{1}{3}\frac{\partial \hat{D}_{\text{eff}}}{\partial \hat{\mathbf{C}}} : \hat{\mathbf{C}}\hat{\mathbf{C}}^{-1}\right] = 2\left[\frac{1}{J}\right]^{\frac{2}{3}} \text{DEV}\frac{\partial \hat{D}_{\text{eff}}}{\partial \hat{\mathbf{C}}} \tag{37}$$

2.3.2. Example of the bi-logarithmic potential. In this paper we will focus on bi-logarithmic potentials that are well suited to simulate metal models. These models also have interesting properties allowing for simpler expressions in the forthcoming developments, as was illustrated in [25]. In elasticity, volumic and deviatoric internal energy are obtained from

$$\Phi^{\text{vol}}(\theta^e) \equiv \frac{K_0}{2}\left[\ln(\theta^e)\right]^2 \quad \text{and} \quad \hat{D}_{\text{eff}}\left(\hat{\mathbf{C}}\right) \equiv \frac{G_0}{4}\ln\left(\hat{\mathbf{C}}\right) : \ln\left(\hat{\mathbf{C}}\right) \tag{38}$$

with K_0 the initial bulk modulus and with G_0 the initial shear modulus.

Pressure (35) is directly computed by

$$p^e = \frac{\partial \Phi^{\text{vol}}(\theta^e)}{\partial \theta^e} = K_0 \frac{\ln(\theta^e)}{\theta^e} \tag{39}$$

The deviatoric stresses are obtained from a spectral decomposition of $\hat{\mathbf{C}}$ into eigenvalues $\lambda^{(\alpha)}$ and eigenvectors $\vec{e}^{(\alpha)}$

$$\hat{\mathbf{C}} = \sum_{\alpha=1}^{3} \left\{\lambda^{(\alpha)} \vec{e}^{(\alpha)} \otimes \vec{e}^{(\alpha)}\right\} \tag{40}$$

leading to

$$\frac{\partial \hat{D}_{\text{eff}}\left(\vec{x}_0, \hat{\mathbf{C}}\right)}{\partial \hat{\mathbf{C}}} = \frac{G_0}{2}\sum_{\alpha=1}^{3}\left\{\frac{\ln \lambda^{(\alpha)}}{\lambda^{(\alpha)}} \vec{e}^{(\alpha)} \otimes \vec{e}^{(\alpha)}\right\} \tag{41}$$

Now, we will expose how to adapt these potentials (and resulting stress) for an elasto-plastic formulation.

3. THE VARIATIONAL FORMULATION OF ELASTO-PLASTICITY UPDATES

In this section we recall the main lines of the variational formulation of visco-plastic updates proposed by Ortiz and Stainier [25]. Next we will particularize these expressions to an elasto-plastic model based on a bi-logarithmic potential with isotropic hardening.

3.1. Hypothesis and definitions

The strain tensor (1) is multiplicatively decomposed into a plastic part $\mathbf{F^{pl}}$ and into an elastic part $\mathbf{F^{el}}$ as

$$\mathbf{F} \quad = \quad \mathbf{F^{el}}\mathbf{F^{pl}} \tag{42}$$

Let $\Phi^{\mathrm{el}}\left(\mathbf{F^{el}}\right)$ be the elastic potential and let $\Phi^{\mathrm{pl}}\left(\mathbf{F^{pl}}\left(Q\right),Q\right)$ be the plastic potential, depending on plastic deformations but also on n internal variables $Q^{(\alpha)} \in \mathbb{R}^n$. A flow rule couples the plastic deformation to the internal variable by

$$\dot{\mathbf{F}}^{\mathbf{pl}} = \dot{Q}^{(\alpha)}\mathbf{N}^{(\alpha)}\mathbf{F^{pl}} \tag{43}$$

where $\mathbf{N}^{(\alpha)}$ is the flow direction corresponding to value $Q^{(\alpha)}$. In the particular case of a von Mises flow rule with only one internal variable, one has [25]

$$Q = \varepsilon^{\mathrm{pl}} \quad \text{and } \mathrm{tr}\mathbf{N} = 0 \quad \text{and } \mathbf{N}:\mathbf{N} = \frac{3}{2} \tag{44}$$

where $\varepsilon^{\mathrm{pl}}$ corresponds to the equivalent plastic strain. In the following, we will assume this flow rule to hold .

Helmholtz free energy function A is therefore rewritten as

$$A\left(\mathbf{F},\mathbf{F^{pl}},\varepsilon^{\mathrm{pl}}\right) \quad \equiv \quad \Phi^{\mathrm{el}}\left(\mathbf{F}\mathbf{F^{pl}}^{-1}\right) + \Phi^{\mathrm{pl}}\left(\mathbf{F^{pl}}\left(\varepsilon^{\mathrm{pl}}\right),\varepsilon^{\mathrm{pl}}\right) \tag{45}$$

From this free energy, the first Piola-Kirchhoff stress tensor $\mathbf{P}$ is obtained by

$$\mathbf{P} \quad \equiv \quad \frac{\partial A\left(\mathbf{F},\mathbf{F^{pl}},\varepsilon^{\mathrm{pl}}\right)}{\partial \mathbf{F}} = \frac{\partial \Phi^{\mathrm{el}}\left(\mathbf{F}\mathbf{F^{pl}}^{-1}\right)}{\partial \mathbf{F}} = A_{,\mathbf{F}} \tag{46}$$

Let $\mathbf{T}$ be the force conjugated to $\mathbf{F^{pl}}$ and let Y be the force conjugated to $\varepsilon^{\mathrm{pl}}$, with

$$\mathbf{T} \equiv -\frac{\partial A\left(\mathbf{F}, \mathbf{F^{pl}}, \varepsilon^{\mathrm{pl}}\right)}{\partial \mathbf{F^{pl}}} = -A_{,\mathbf{F^{pl}}} \quad \text{and} \quad Y \equiv -\frac{\partial A\left(\mathbf{F}, \mathbf{F^{pl}}, \varepsilon^{\mathrm{pl}}\right)}{\partial \varepsilon^{\mathrm{pl}}} \tag{47}$$

Let Ψ be a dissipation pseudo potential associated to $\dot{\varepsilon}^{\mathrm{pl}}$ such that

$$\dot{\varepsilon}^{\mathrm{pl}} = \frac{\partial \Psi\left(Y\right)}{\partial Y} = \Psi_{,Y} \tag{48}$$

A Legendre mapping leads to the dual potential Ψ^* with

$$\Psi^*\left(\dot{\varepsilon}^{\mathrm{pl}}\right) = \sup_{Y}\left(Y\dot{\varepsilon}^{\mathrm{pl}} - \Psi\left(Y\right)\right) \quad \text{and} \quad Y = \frac{\partial \Psi^*\left(\dot{\varepsilon}^{\mathrm{pl}}\right)}{\partial \dot{\varepsilon}^{\mathrm{pl}}} = \Psi^*_{,\dot{\varepsilon}^{\mathrm{pl}}} \tag{49}$$

If Ψ is convex, with $\Psi\left(0\right) = 0$, it leads to the property $\dot{\varepsilon}^{\mathrm{pl}} > 0$ if Y remains positive. The hypothesis of a Perzyna model leads to

$$\Psi^* = \begin{cases} \frac{mY_0\dot{\varepsilon}_0^{\mathrm{pl}}}{m+1}\left[\frac{\dot{\varepsilon}^{\mathrm{pl}}}{\dot{\varepsilon}_0^{\mathrm{pl}}}\right]^{\frac{m+1}{m}} & \text{if} \dot{\varepsilon}^{\mathrm{pl}} \geq 0 \\ \infty & \text{if} \dot{\varepsilon}^{\mathrm{pl}} < 0 \end{cases} \tag{50}$$

where Y_0, $\dot{\varepsilon}_0^{\mathrm{pl}}$ and m are constants. Particular choice of $m \to \infty$ yields

$$\Psi^* = \begin{cases} Y_0\dot{\varepsilon}^{\mathrm{pl}} & \text{if} \dot{\varepsilon}^{\mathrm{pl}} \geq 0 \\ \infty & \text{if} \dot{\varepsilon}^{\mathrm{pl}} < 0 \end{cases} \tag{51}$$

that will ensure the elasto-plastic flow occurs with $\dot{\varepsilon}^{\mathrm{pl}} > 0$.

Let us now establish some basic relations. Using (42), (43) and (45), forces $\mathbf{T}$ and Y (47) can be rewritten as

$$\begin{aligned} \mathbf{T} &= \mathbf{F^{el}}^T\mathbf{P} - \underbrace{\frac{\partial \Phi^{\mathrm{pl}}\left(\mathbf{F^{pl}}, \varepsilon^{\mathrm{pl}}\right)}{\partial \mathbf{F^{pl}}}}_{\equiv \mathbf{T_c}} \\ Y &= -\frac{\partial A\left(\mathbf{F}, \mathbf{F^{pl}}, \varepsilon^{\mathrm{pl}}\right)}{\partial \mathbf{F^{pl}}} : \frac{\partial \mathbf{F^{pl}}}{\partial \varepsilon^{\mathrm{pl}}} - \underbrace{\frac{\partial A\left(\varepsilon^{\mathrm{pl}}\right)}{\partial \varepsilon^{\mathrm{pl}}}}_{\equiv A_{,\varepsilon^{\mathrm{pl}}}} = \mathbf{T} : \left[\mathbf{N}\mathbf{F^{pl}}\right] - A_{,\varepsilon^{\mathrm{pl}}} \end{aligned} \tag{52}$$

where $\mathbf{T_c}$ is therefore the backstress tensor and where $A_{,\varepsilon^{\mathrm{pl}}}$ comes from the explicit dependence of A to $\varepsilon^{\mathrm{pl}}$.

3.2. Continuous dynamics

Using the free energy function A (45) with three new independent variables, Ortiz and Stainier [25] proposed the following expression of a functional

$$D\left(\dot{\mathbf{F}},\dot{\varepsilon}^{\mathrm{pl}},\mathbf{N}\right) \equiv \frac{\partial A}{\partial \mathbf{F}}:\dot{\mathbf{F}}-Y\dot{\varepsilon}^{\mathrm{pl}}+\Psi^*\left(\dot{\varepsilon}^{\mathrm{pl}}\right) \tag{53}$$

3.2.1. Differentiation with respect to $\dot{\varepsilon}^{pl}$. Using (51) yields

$$\frac{\partial D\left(\dot{\mathbf{F}},\dot{\varepsilon}^{\mathrm{pl}},\mathbf{N}\right)}{\partial \dot{\varepsilon}^{\mathrm{pl}}} = -Y+\frac{\partial \Psi^*}{\partial \dot{\varepsilon}^{\mathrm{pl}}}=0 \tag{54}$$

demonstrating D must be minimum with respect to $\dot{\varepsilon}^{\mathrm{pl}}$.

3.2.2. Differentiation with respect to $\mathbf{N}$. Functional D depends on $\mathbf{N}$ through term Y. Using relation (52) leads to

$$\frac{\partial D\left(\dot{\mathbf{F}},\dot{\varepsilon}^{\mathrm{pl}},\mathbf{N}\right)}{\partial \mathbf{N}} = -\frac{\partial \dot{\varepsilon}^{\mathrm{pl}}\mathbf{T}:\mathbf{N}\mathbf{F}^{\mathbf{pl}}}{\partial \mathbf{N}} \tag{55}$$

Assuming the functional is minimum related to the flow direction $\mathbf{N}$ under constraints (44) leads to a flow direction oriented along the deviatoric stress, that is consistent with the usual models of plasticity. Indeed, using (44), and introducing Langrangian multipliers λ_1 and λ_2, minimisation of D becomes

$$\min_{\mathbf{N},\lambda_1,\lambda_2}\left(-\mathbf{T}{\mathbf{F}^{\mathbf{pl}}}^T:\mathbf{N}+\lambda_1\mathrm{tr}\mathbf{N}+\lambda_2\left[\mathbf{N}:\mathbf{N}-\frac{3}{2}\right]\right) \tag{56}$$

Differentiation with respect to $\mathbf{N}$ leads to

$$0=-\mathbf{T}{\mathbf{F}^{\mathbf{pl}}}^T+\lambda_1\mathbf{I}+2\lambda_2\mathbf{N} \quad\Leftrightarrow\quad \lambda_1=\frac{1}{3}\mathrm{tr}\left(\mathbf{T}{\mathbf{F}^{\mathbf{pl}}}^T\right) \tag{57}$$

Therefore $\mathbf{N}$ is oriented along $\mathrm{dev}\left(\mathbf{T}{\mathbf{F}^{\mathbf{pl}}}^T\right)$, and since $\mathbf{N}:\mathbf{N}=\frac{3}{2}$, it yields

$$\mathbf{N} = \sqrt{\frac{3}{2}}\frac{\mathrm{dev}\left(\mathbf{T}{\mathbf{F}^{\mathbf{pl}}}^T\right)}{\sqrt{\mathrm{dev}\left(\mathbf{T}{\mathbf{F}^{\mathbf{pl}}}^T\right):\mathrm{dev}\left(\mathbf{T}{\mathbf{F}^{\mathbf{pl}}}^T\right)}} \tag{58}$$

Therefore D, constrained by (44) must be minimum with respect to $\mathbf{N}$.

3.2.3. Differentiation with respect to $\dot{\mathbf{F}}$. If we identify the effective potential D_{eff} to the minimum of D related to $\dot{\varepsilon}^{\text{pl}}$ and $\mathbf{N}$

$$D_{\text{eff}}\left(\dot{\mathbf{F}}\right) \equiv \min_{\dot{\varepsilon}^{\text{pl}},\mathbf{N}} D\left(\dot{\mathbf{F}},\dot{\varepsilon}^{\text{pl}},\mathbf{N}\right) \tag{59}$$

using (46) and (53) leads to

$$\frac{\partial D_{\text{eff}}\left(\dot{\mathbf{F}}\right)}{\partial \dot{\mathbf{F}}} = \frac{\partial A}{\partial \mathbf{F}} = \mathbf{P} \tag{60}$$

This relation demonstrates that the stress tensor (here the first Piola-Kirchhoff, but it remains also true for the second Piola-Kirchhoff one) derives from a rate potential even if plasticity occurs, as assumed in relation (19).

3.3. Incremental formulation: elasto-plastic updates

Let us assume a time increment Δt from configuration n to configuration $n+1$. Integration of relation (43) using relation (44), leads to [25]

$$\mathbf{F^{pl}}^{n+1} = \underbrace{\exp\left(\left[{\varepsilon^{\text{pl}}}^{n+1} - {\varepsilon^{\text{pl}}}^{n}\right]\mathbf{N}\right)}_{\equiv\mathbf{A}\left({\varepsilon^{\text{pl}}}^{n+1}-{\varepsilon^{\text{pl}}}^{n}\right)} \mathbf{F^{pl}}^{n} \tag{61}$$

where tensor $\mathbf{A}$ has the following properties

$$\det\mathbf{A} = \exp\text{tr}\left(\Delta\varepsilon^{\text{pl}}\mathbf{N}\right) = 1 \quad \text{and} \quad \Delta\varepsilon^{\text{pl}} = \sqrt{\frac{2}{3}\ln\mathbf{A} : \ln\mathbf{A}} \tag{62}$$

with $\Delta\varepsilon^{\text{pl}} = {\varepsilon^{\text{pl}}}^{n+1} - {\varepsilon^{\text{pl}}}^{n}$.

Time integration of functional D (53) leads to

$$\begin{aligned}\Delta D\left(\mathbf{F}^{n+1},\mathbf{F}^{n},{\varepsilon^{\text{pl}}}^{n+1},{\varepsilon^{\text{pl}}}^{n},\mathbf{N}\right) \equiv A\left(\mathbf{F}^{n+1},\mathbf{F^{pl}}^{n+1}\left({\varepsilon^{\text{pl}}}^{n+1}\right),{\varepsilon^{\text{pl}}}^{n+1}\right) - \\ A\left(\mathbf{F}^{n},\mathbf{F^{pl}}^{n}\left({\varepsilon^{\text{pl}}}^{n}\right),{\varepsilon^{\text{pl}}}^{n}\right) + \Delta t\Psi^{*}\left(\frac{{\varepsilon^{\text{pl}}}^{n+1}-{\varepsilon^{\text{pl}}}^{n}}{\Delta t}\right)\end{aligned} \tag{63}$$

with A defined by (45) and Ψ^{*} defined by (49).

3.3.1. Differentiation with respect to ${\varepsilon^{pl}}^{n+1}$. Using (47) and (49) yields

$$\frac{\partial \Delta D}{\partial {\varepsilon^{\mathrm{pl}}}^{n+1}} = \frac{\partial A\left(\mathbf{F}^{n+1}, {\mathbf{F}^{\mathbf{pl}}}^{n+1}\left({\varepsilon^{\mathrm{pl}}}^{n+1}\right), {\varepsilon^{\mathrm{pl}}}^{n+1}\right)}{\partial {\varepsilon^{\mathrm{pl}}}^{n+1}} + \frac{\partial \Psi^*}{\partial {\varepsilon^{\mathrm{pl}}}^{n+1}} = -Y + \frac{\partial \Psi^*}{\partial \dot{\varepsilon}^{\mathrm{pl}}} = 0 \quad (64)$$

demonstrating ΔD must be minimum with respect to ${\varepsilon^{\mathrm{pl}}}^{n+1}$.

3.3.2. Differentiation with respect to $\mathbf{N}$. Functional ΔD depends on $\mathbf{N}$ through $\mathbf{F^{pl}}$. Using relation (47), relation (61) leads to

$$\frac{\partial \Delta D}{\partial \mathbf{N}} = \frac{\partial A\left(\mathbf{F}^{n+1}, {\mathbf{F}^{\mathbf{pl}}}^{n+1}\left({\varepsilon^{\mathrm{pl}}}^{n+1}\right), {\varepsilon^{\mathrm{pl}}}^{n+1}\right)}{\partial {\mathbf{F}^{\mathbf{pl}}}^{n+1}} : \frac{\partial {\mathbf{F}^{\mathbf{pl}}}^{n+1}}{\partial \mathbf{N}} = -\mathbf{T} : \left[\frac{\partial \mathbf{A}}{\partial \mathbf{N}}\mathbf{F}^{\mathbf{pl}^n}\right] \quad (65)$$

Assuming ΔD must be minimum with respect to the flow direction $\mathbf{N}$ leads, under some assumptions, to a radial return mapping scheme as we will see in the next section.

3.3.3. Differentiation with respect to $\mathbf{F}^{n+1}$. Assuming sufficient convexity properties for the physical potentials A and Ψ^*, the stationary point of ΔD will correspond to a minimum. Therefore, the effective incremental potential ΔD_{eff} is identified to this minimum of ΔD with respect to ${\varepsilon^{\mathrm{pl}}}^{n+1}$ and $\mathbf{N}$

$$\Delta D_{\mathrm{eff}}\left(\mathbf{F}\right) \equiv \min_{{\varepsilon^{\mathrm{pl}}}^{n+1}, \mathbf{N}} \Delta D\left(\mathbf{F}^{n+1}, \mathbf{F}^n, {\varepsilon^{\mathrm{pl}}}^{n+1}, {\varepsilon^{\mathrm{pl}}}^n, \mathbf{N}\right) \quad (66)$$

Using relations (46) and (63) leads to

$$\frac{\partial \Delta D_{\mathrm{eff}}\left(\mathbf{F}^{n+1}\right)}{\partial \mathbf{F}^{n+1}} = \frac{\partial A\left(\mathbf{F}^{n+1}\right)}{\partial \mathbf{F}^{n+1}} = \mathbf{P}^{n+1} \quad (67)$$

This relation demonstrates that, even when plasticity occurs, the stress tensor derives from an incremental potential.

When adapting these relations to the particular case of bi-logarithmic potentials and isotropic hardening, one can find:

$$\mathbf{PK}^{n+1} = p^e J\left[\mathbf{C}^{n+1}\right]^{-1} + \underbrace{2\left[\frac{1}{J}\right]^{\frac{2}{3}} \mathrm{DEV}\left(\mathbf{f}^{\mathbf{pl}^{n+1}} \frac{\partial \hat{\Phi}^{\mathrm{el}}\left(\hat{\mathbf{C}}^{\mathbf{el}}\right)}{\partial \hat{\mathbf{C}}^{\mathbf{el}}} \mathbf{f}^{\mathbf{pl}^{n+1^T}}\right)}_{=\frac{\partial \widetilde{\Delta D}_{\mathrm{eff}}}{\partial \mathbf{C}}} \quad (68)$$

with $\hat{\Phi}^{\text{el}}\left(\hat{\mathbf{C}}^{\mathbf{el}}\right)$ the deviatoric part of the elastic potential. Details of this evaluation can be found in appendix I.

Now we will use this variational formalism to design an energy-momentum conserving time integration algorithm.

4. THE ENERGY MOMENTUM CONSERVING ALGORITHM (EMCA)

Once the balance relation (30) is established for a given time t, this relation must be integrated in time. To achieve this goal, Simo and Tarnow [6] proposed the EMCA. In this section we will present the main features of the EMCA algorithm. Next we will deduce the conditions on the forces resulting from the conservations laws expressed by relations (13), (15) and (21).

4.1. Description of the EMCA

The relation between positions and velocities at node ξ is

$$\left[\vec{x}^{n+1}\right]^{\xi} = \left[\vec{x}^{n}\right]^{\xi} + \frac{\Delta t}{2}\left[\dot{\vec{x}}^{n+1}\right]^{\xi} + \frac{\Delta t}{2}\left[\dot{\vec{x}}^{n}\right]^{\xi} \tag{69}$$

This relation is a second order approximation (in Δt). A second order approximation of the relations between the velocities and the accelerations at node ξ is

$$\left[\dot{\vec{x}}^{n+1}\right]^{\xi} = \left[\dot{\vec{x}}^{n}\right]^{\xi} + \frac{\Delta t}{2}\left[\ddot{\vec{x}}^{n+1}\right]^{\xi} + \frac{\Delta t}{2}\left[\ddot{\vec{x}}^{n}\right]^{\xi} \tag{70}$$

The balance relation (30) is discretized in time at node ξ by

$$\frac{1}{2}M^{\xi\mu}\left[\ddot{\vec{x}}^{n+1} + \ddot{\vec{x}}^{n}\right]^{\mu} = \left[\vec{F}_{\text{ext}}^{n+\frac{1}{2}} - \vec{F}_{\text{int}}^{n+\frac{1}{2}}\right]^{\xi} \tag{71}$$

This relation is a second order approximation of relation (30) if the internal forces $\vec{F}_{\text{int}}^{n+\frac{1}{2}}$ are a second order approximation of $\vec{F}_{\text{int}}\left(t^{n+\frac{1}{2}}\right)$. The set of relations (69), (70) and (71) is solved

by a predictor-corrector algorithm enhanced with a line search resolution [33, page 254].

4.2. Verification of conservation laws

In this section we will verify the conservation laws expressed by relations (13), (15) and (21).

4.2.1. Conservation of linear momentum. A sum on ξ in relation (71) and the use of relation (70) leads to

$$\underbrace{\sum_{\xi} M^{\xi\mu}\left[\dot{\vec{x}}^{n+1}\right]^{\mu}}_{\vec{L}^{n+1}} - \underbrace{\sum_{\xi} M^{\xi\mu}\left[\dot{\vec{x}}^{n}\right]^{\mu}}_{\vec{L}^{n}} = \Delta t \sum_{\xi}\left[\vec{F}_{\text{ext}}^{n+\frac{1}{2}} - \vec{F}_{\text{int}}^{n+\frac{1}{2}}\right]^{\xi} \tag{72}$$

where the continuous linear momentum $\vec{L}$ defined by relation (12) is discretized thanks to relation (7) in $\vec{L} = \sum_{\xi} M^{\xi\mu}\dot{\vec{x}}^{\mu}$. Relation (72) is a time discretization of relation (13) if

$$\sum_{\xi}\left[\vec{F}_{\text{int}}^{n+\frac{1}{2}}\right]^{\xi} = 0 \tag{73}$$

4.2.2. Conservation of angular momentum. Thanks to relations (69) and (70), the vector product between $\vec{x}^{n+\frac{1}{2}} = \frac{\vec{x}^{n}+\vec{x}^{n+1}}{2}$ and relation (71) leads to

$$\begin{aligned}\frac{1}{\Delta t}\underbrace{M^{\xi\mu}\left[\vec{x}^{n+1}\right]^{\xi} \wedge \left[\dot{\vec{x}}^{n+1}\right]^{\mu}}_{\vec{J}^{n+1}} - \frac{1}{\Delta t}\underbrace{M^{\xi\mu}\left[\vec{x}^{n}\right]^{\xi} \wedge \left[\dot{\vec{x}}^{n}\right]^{\mu}}_{\vec{J}^{n}} = \\ \left[\vec{x}^{n+\frac{1}{2}}\right]^{\xi} \wedge \left[\vec{F}_{\text{ext}}^{n+\frac{1}{2}} - \vec{F}_{\text{int}}^{n+\frac{1}{2}}\right]^{\xi}\end{aligned} \tag{74}$$

where the continuous angular momentum $\vec{J}$ defined by relation (14) is discretized thanks to relation (7) in $\vec{J} = M^{\xi\mu}\vec{x}^{\xi} \wedge \dot{\vec{x}}^{\mu}$. Therefore, relation (74) is a discretization of (14) if

$$\left[\frac{\vec{x}^{n+1}+\vec{x}^{n}}{2}\right]^{\xi} \wedge \left[\vec{F}_{\text{int}}^{n+\frac{1}{2}}\right]^{\xi} = 0 \tag{75}$$

4.2.3. Conservation of energy. Thanks to relations (69) and (70), the dot product between $\dot{\vec{x}}^{n+\frac{1}{2}} = \frac{\dot{\vec{x}}^n + \dot{\vec{x}}^{n+1}}{2}$ and relation (71) leads to

$$\underbrace{\frac{M^{\xi\mu}}{2}\left[\dot{\vec{x}}^{n+1}\right]^\xi \cdot \left[\dot{\vec{x}}^{n+1}\right]^\mu}_{K^{n+1}} - \underbrace{\frac{M^{\xi\mu}}{2}\left[\dot{\vec{x}}^{n}\right]^\xi \cdot \left[\dot{\vec{x}}^{n}\right]^\mu}_{K^{n}} + \left[\vec{x}^{n+1} - \vec{x}^n\right]^\xi \cdot \left[\vec{F}_{\rm int}^{n+\frac{1}{2}}\right]^\xi = \underbrace{\left[\vec{x}^{n+1} - \vec{x}^n\right]^\xi \cdot \left[\vec{F}_{\rm ext}^{n+\frac{1}{2}}\right]^\xi}_{W_{\rm ext}^{n+1} - W_{\rm ext}^n} \tag{76}$$

where the continuous kinetic energy K defined in relation (16) is dicretized thanks to relation (7) in $K = \frac{1}{2}M^{\xi\mu}\dot{x}^\xi \cdot \dot{x}^\mu$ and where the power of the external forces $\dot{W}_{\rm ext}$ defined in relation (16) is discretized and integrated in $W_{\rm ext}^{n+1} - W_{\rm ext}^n = \left[\vec{x}^{n+1} - \vec{x}^n\right]^\xi \cdot \left[\vec{F}_{\rm ext}^{n+\frac{1}{2}}\right]^\xi$. Let E be the discretized energy, let $W^{\rm el}$ be the discretized reversible energy, let $W^{\rm pl}$ be the discretized irreversible energy and let $D_{\rm eff}$ be the discretized effective potential. Let us define

$$\begin{aligned} \Delta W^{\rm el} &= \int_{\mathbb{V}_0} \left\{\Delta\Phi^{\rm el}\right\} d\mathbb{V}_0 \\ \Delta W^{\rm pl} &= \int_{\mathbb{V}_0} \left\{\Delta\Phi^{\rm pl} + \Delta t \Psi^*\right\} d\mathbb{V}_0 \end{aligned} \tag{77}$$

Therefore relation (21) can be discretized into

$$K^{n+1} - K^n + \underbrace{\left[W^{\rm el} + W^{\rm pl}\right]^{n+1} - \left[W^{\rm el} + W^{\rm pl}\right]^n}_{= \int_{\mathbb{V}_0}\left\{D_{\rm eff}^{n+1} - D_{\rm eff}^n\right\} d\mathbb{V}_0} = W_{\rm ext}^{n+1} - W_{\rm ext}^n \tag{78}$$

If this last expression is compared with relation (76), the internal forces must lead to

$$\left[\vec{F}_{\rm int}^{n+\frac{1}{2}}\right]^\xi \cdot \left[\vec{x}^{n+1} - \vec{x}^n\right]^\xi = \int_{\mathbb{V}_0} \left\{D_{\rm eff}^{n+1} - D_{\rm eff}^n\right\} d\mathbb{V}_0 = \int_{\mathbb{V}_0} \left\{\Delta D_{\rm eff}\right\} d\mathbb{V}_0 \tag{79}$$

The challenge of the EMCA algorithm is to find a consistent expression of the internal forces and of the dissipation terms that satisfies relations (73), (75) and (79). This will be the topic of the next section.

4.3. Internal formulation of the internal forces

Let us extend the general formulation of the second Piola-Kirchhoff stress tensor proposed by Gonzalez [8] for hyper-elasticity to our elasto-plastic formulation. Gonzalez [8] defined modified values to reach the conservation of the thermodynamics laws. Let $\hat{\mathbf{PK}}^{n+\frac{1}{2}}$ be the modified deviatoric stresses and let $p^{n+\frac{1}{2}}$ be the modified pressure. Let the internal forces be

$$\left[\vec{F}_{\text{int}}^{n+\frac{1}{2}}\right]^{\xi} = \int_{\mathbb{V}_0} \left\{ \frac{\mathbf{F}^{n+1}+\mathbf{F}^n}{2} \left[\hat{\mathbf{PK}}^{n+\frac{1}{2}} + 2p^{n+\frac{1}{2}}\mathbf{dG} \right] \vec{D}^{\xi} \right\} d\mathbb{V}_0 \tag{80}$$

with $\mathbf{dG}$ the modified differentiation of J by $\mathbf{C}$. Let us use the split of ΔD_{eff} defined by relations (106) and (107).

Therefore the general expression proposed by Gonzalez [8] can be rewritten by using the variational formulation of elasto-plastic updates. The modified differentiation of J becomes

$$\begin{aligned} \mathbf{dG} &= \mathbf{DG}^{n+\frac{1}{2}} + \left[\frac{J^{n+1} - J^n - \mathbf{DG}^{n+\frac{1}{2}} : \mathbf{\Delta C}}{\|\mathbf{\Delta C}\|^2} \right] \mathbf{\Delta C} \\ \mathbf{DG}^{n+\frac{1}{2}} &= \frac{1}{2}\sqrt{\det\left(\frac{\mathbf{C}^{n+1}+\mathbf{C}^n}{2}\right)} \left[\frac{\mathbf{C}^{n+1}+\mathbf{C}^n}{2}\right]^{-1} \\ \mathbf{\Delta C} &= \mathbf{C}^{n+1} - \mathbf{C}^n \end{aligned} \tag{81}$$

while the modified pressure becomes

$$\begin{aligned} p^{n+\frac{1}{2}} &= \frac{\partial U^{\text{vol}}}{\partial \theta^e}^{\frac{n+1}{2}} + \left[\frac{U^{\text{vol}}\left(\theta^{e\,n+1}\right) - U^{\text{vol}}\left(\theta^{e\,n}\right) - \frac{\partial U^{\text{vol}}}{\partial \theta^e}^{\frac{n+1}{2}} \Delta\theta^e}{|\Delta\theta^e|^2} \right] \Delta\theta^e \\ \frac{\partial U^{\text{vol}}}{\partial \theta^e}^{\frac{n+1}{2}} &= \frac{\partial U^{\text{vol}}}{\partial \theta^e}\left(\frac{\theta^{e\,n+1}+\theta^{e\,n}}{2}\right) \\ \Delta\theta^e &= \theta^{e\,n+1} - \theta^{e\,n} \end{aligned} \tag{82}$$

Modified deviatoric stresses are obtained by

$$\begin{aligned}
\hat{\mathbf{PK}}^{n+\frac{1}{2}} &= 2\mathbf{D}\widehat{\mathbf{\Delta D}}_{\text{eff}}^{\,n+\frac{1}{2}} + 2\left[\frac{\widehat{\Delta D}_{\text{eff}}\left(\mathbf{C}^{n+1},\mathbf{C}^{n}\right) - \mathbf{D}\widehat{\mathbf{\Delta D}}_{\text{eff}}^{\,n+\frac{1}{2}} : \mathbf{\Delta C}}{\|\mathbf{\Delta C}\|^2}\right]\mathbf{\Delta C} \\
\mathbf{D}\widehat{\mathbf{\Delta D}}_{\text{eff}}^{\,n+\frac{1}{2}} &= \frac{\partial \widehat{\Delta D}_{\text{eff}}}{\partial \mathbf{C}}\left(\frac{\mathbf{C}^{n+1}+\mathbf{C}^{n}}{2}\right) \\
\mathbf{\Delta C} &= \mathbf{C}^{n+1}-\mathbf{C}^{n}
\end{aligned} \tag{83}$$

In this last expression, $\frac{\partial \widehat{\Delta D}_{\text{eff}}}{\partial \mathbf{C}}\left(\frac{\mathbf{C}^{n+1}+\mathbf{C}^{n}}{2}\right)$ is obtained as the deviatoric part of relation (68), *i.e.*

$$\frac{\partial \widehat{\Delta D}_{\text{eff}}}{\partial \mathbf{C}} = 2\left[\frac{1}{J}\right]^{\frac{2}{3}} \text{DEV}\left(\mathbf{f^{pl}}\frac{\partial \hat{\Phi}^{\text{el}}\left(\hat{\mathbf{C}}^{\mathbf{el}}\right)}{\partial \hat{\mathbf{C}}^{\mathbf{el}}}\mathbf{f^{pl}}^{T}\right) \tag{84}$$

Let us draw some remarks:

(i) This method requires to compute the effective potential for $\frac{\mathbf{C}^{n+1}+\mathbf{C}^{n}}{2}$ and also for $\mathbf{C}^{n+1}$.

(ii) These expressions lead to a second order approximation of the internal forces computed in the mid-configuration (*i.e.* $\vec{F}_{\text{int}}\left(\frac{\vec{x}^{n+1}+\vec{x}^{n}}{2}\right)$) [8]. Let us note that using the internal forces computed in the mid-configuration introduces a coupling between rotation and stretches. This coupling introduces some instabilities [34].

(iii) These expressions are valid for any formulation using the variational formulation.

(iv) Expression of the consistent stiffness matrix $\mathbf{K} = \frac{\partial \vec{F}_{\text{int}}^{\,n+\frac{1}{2}}}{\partial \vec{x}^{n+1}}$ associated to internal forces can be found in appendix II. The resulting expression is

$$\begin{aligned}
\mathbf{K}_{ik}^{\xi\mu} = &\int_{\mathbb{V}_0}\left\{\vec{D}_j^{\xi}\mathcal{G}_{ijkl}\vec{D}_l^{\xi}\right\}d\mathbb{V}_0 + \int_{\mathbb{V}_0}\left\{\vec{D}_j^{\xi}\mathcal{H}_{ijkl}^{\text{vol1}}\frac{1}{\mathbb{V}_0}\int_{\mathbb{V}_0}\left\{J\mathbf{f}^{n+1}{}^{T}_{lp}\vec{D}_p^{\mu}\right\}d\mathbb{V}_0\right\}d\mathbb{V}_0 + \\
&\int_{\mathbb{V}_0}\left\{\vec{D}_j^{\xi}\mathcal{H}_{ijkl}^{\text{vol2}}\vec{D}_l^{\mu}\right\} + \int_{\mathbb{V}_0}\left\{\vec{D}_j^{\xi}\mathcal{H}_{ijkl}^{\text{dev}}\vec{D}_l^{\mu}\right\}d\mathbb{V}_0
\end{aligned} \tag{85}$$

where $\mathcal{G}$ results from the geometric part, where $\mathcal{H}^{\text{vol1}}$ results form the differentiation of the pressure, where $\mathcal{H}^{\text{vol2}}$ results from the differentiation of the differentiation of J and where $\mathcal{H}^{\text{dev}}$ results from the differentiation of the deviatoric stresses. These tensors are

evaluated in appendix II. Unfortunately $\mathcal{H}_{ijkl} \neq \mathcal{H}_{kjil}$, leading to a non-symmetrical stiffness.

Now let us demonstrate that the expression (80) of the internal forces satisfies the conservation laws (73), (75) and (79).

4.3.1. Conservation of linear momentum. Using properties of the shape functions, a sum on ξ in relation (80) leads to

$$\sum_{\xi} \left[\vec{F}_{\text{int}}^{n+\frac{1}{2}}\right]^{\xi} = \int_{\mathbb{V}_0} \left\{ \frac{\mathbf{F}^{n+1}+\mathbf{F}^{n}}{2} \left[\hat{\mathbf{PK}}^{n+\frac{1}{2}} + 2p^{n+\frac{1}{2}}\mathbf{dG}\right] \underbrace{\sum_{\xi} \vec{D}^{\xi}}_{=0} \right\} d\mathbb{V}_0 = 0 \qquad (86)$$

4.3.2. Conservation of angular momentum. Using the symmetry properties of $\hat{\mathbf{PK}}$ and of $\mathbf{dG}$, relation (80) leads to

$$\left[\frac{\vec{x}^{n+1}+\vec{x}^{n}}{2}\right]^{\xi} \wedge \left[\vec{F}_{\text{int}}^{n+\frac{1}{2}}\right]^{\xi} = \int_{\mathbb{V}_0} \left\{ \epsilon : \left[\frac{\mathbf{F}^{n+1}+\mathbf{F}^{n}}{2} \left[\hat{\mathbf{PK}}^{n+\frac{1}{2}} + 2p^{n+\frac{1}{2}}\mathbf{dG}\right] \frac{\left[\mathbf{F}^{n+1}+\mathbf{F}^{n}\right]^{T}}{2} \right] \right\} d\mathbb{V}_0 = 0 \qquad (87)$$

where ϵ is the third order permutation tensor. This expression is equal to zero since $[\epsilon : \mathbf{A}]_i = \epsilon_{ijk} : \mathbf{A}_{jk}$ is always equal to zero if $\mathbf{A}$ is symmetric.

4.3.3. Conservation of energy. Using the symmetry properties of $\hat{\mathbf{PK}}$ and of $\mathbf{dG}$, relations (80), (81) and (83) lead to

$$\begin{aligned} \left[\vec{F}_{\text{int}}^{n+\frac{1}{2}}\right]^{\xi} \cdot \left[\vec{x}^{n+1}-\vec{x}^{n}\right]^{\xi} &= \int_{\mathbb{V}_0} \left\{ \frac{\mathbf{C}^{n+1}-\mathbf{C}^{n}}{2} : \left[\hat{\mathbf{PK}}^{n+\frac{1}{2}} + 2p^{n+\frac{1}{2}}\mathbf{dG}\right] \right\} d\mathbb{V}_0 \\ &= \int_{\mathbb{V}_0} \left\{ \widehat{\Delta D}_{\text{eff}} + p^{n+\frac{1}{2}} \left[J^{n+1}-J^{n}\right] \right\} d\mathbb{V}_0 \end{aligned} \qquad (88)$$

Since $p^{n+\frac{1}{2}}$ is constant over the element, using definition of θ^e (23) and (82) yields

$$\begin{aligned}\left[\vec{F}_{\text{int}}^{n+\frac{1}{2}}\right]^{\xi}\cdot\left[\vec{x}^{n+1}-\vec{x}^{n}\right]^{\xi} &= \int_{\mathbb{V}_0}\left\{\widehat{\Delta D}_{\text{eff}}\right\}d\mathbb{V}_0+p^{n+\frac{1}{2}}\int_{\mathbb{V}_0}\left\{\left[\theta^{en+1}-\theta^{en}\right]\right\}d\mathbb{V}_0\\ &= \int_{\mathbb{V}_0}\left\{\widehat{\Delta D}_{\text{eff}}+U^{\text{vol}}\left(\theta^{en+1}\right)-U^{\text{vol}}\left(\theta^{en}\right)\right\}d\mathbb{V}_0\\ &= \int_{\mathbb{V}_0}\left\{D_{\text{eff}}^{n+1}-D_{\text{eff}}^{n}\right\}d\mathbb{V}_0 \qquad (89)\end{aligned}$$

that satisfies relation (79).

These developments prove that the variational formulation allows us to use the general expression of Gonzalez without modification (except the use of the incremental potential).

5. NUMERICAL EXAMPLES

In this section we will verify that the proposed scheme leads to consistent time integration for numerical applications. Moreover, we will show that the scheme is effectively second order accurate. In the first example we will demonstrate that the proposed scheme is consistent when plastic deformation occurs. Next, we will prove on the Taylor bar problem that an increase of the time step size does not lead to divergence or lack of accuracy, contrarily to the Newmark scheme. Next, we will study a problem exhibiting contact interactions that will confirm the previous observations. Finally a more dramatic example of impact will illustrate the robustness of the code. The finite element discretization considers bilinear 4-node quadrangles with 4 Gauss points for 2-dimensional problems and trilinear 8-node bricks with 8 Gauss points for 3-dimensional problems.

5.1. Numerical example 1: tumbling beam

[Figure 1 about here.]

[Table 1 about here.]

Let us study the tumbling beam proposed by Meng and Laursen [9]. Figure 1 illustrates the geometry of the beam and its properties are reported in Table I. The beam is discretized into 64 quadrangles (4 along the height and 16 along the length). The applied nodal forces Fi (see Figure 1) are described by the equations

$$\begin{aligned} Fi\,(t) = &\quad i * \tfrac{t}{5} \qquad \text{if } 0 \leq t \leq 5s \\ = &\quad i * \tfrac{10-t}{5} \qquad \text{if } 5s < t \leq 10s \end{aligned} \tag{90}$$

and are released after $10s$. The material is assumed to be elastic perfectly plastic. The problem is solved with the EMCA algorithm and a constant time step $\Delta t = 0.5s$.

[Figure 2 about here.]

[Figure 3 about here.]

[Figure 4 about here.]

Figure 2(a) illustrates the time evolution of the angular momentum (around z-axis). During the initial loading ($t \leq 10s$) this value decreases and remains constant during the following computation. When analyzing the energy plastically dissipated (Figure 2(b)) it appears that most of the increase occurs during the loading and that this energy remains almost constant after $100s$. Let us analyse the energy balance. The internal energy and the energy plastically dissipated can be computed from the internal potential at each time step. The finite work of the internal forces is computed by adding the incremental work during each time step:

$$W_{\text{int}}^{n+1} = \sum_{i=0}^{n} \left\{ \vec{F}_{\text{int}}^{i+\frac{1}{2}} \cdot \left[\vec{x}^{i+1} - \vec{x}^{i} \right] \right\} \tag{91}$$

Relation (79) shows that this work must be equal to the sum of the internal energy with the energy plastically dissipated. Figure 3(a) illustrates the balance of the internal energy. It appears that the sum of the internal energy and the plastically dissipated energy is exactly equal to the work done by the internal forces (since the two curves are the same, only a few points of the work of internal forces are represented by a triangle for clarity purpose). Moreover, summing the kinetic energy and the work done by the internal forces (Figure 3(b)) leads to a value exactly equal to the work of the external forces. These observations demonstrate the consistency of the time integration. Finally Figure 4 illustrates the distribution of the equivalent plastic strain. When the external forces are maximum (Figure 4(a)) there is no plastic deformation, when the loading is released (Figure 4(b)) localized plastic strains appear where loads were applied, and after a long time (Figure 4(c)) it appears that there are also plastic strains on the opposite side.

5.2. Numerical example 2: Taylor's bar impact

[Figure 5 about here.]

[Table 2 about here.]

The initial geometry of Taylors's bar is illustrated at Figure 5 and geometrical and material properties are reported in Table II. The bar has an initial velocity $\dot{\vec{x}}_0$ and its lower face is constrained to stay in the plane $z = 0$. The material behavior assumed to be elasto-plastic with linear isotropic hardening. A quarter of the bar is modelled with 576 elements (48 on the base, and 12 along the length). This example was largely studied in the literature (see *e.g.* [35]). It was also studied in the framework of consistent time algorithms for hyper-elastic based elasto-plastic models by Meng and Laursen [10], and in the framework of consistent time

algorithms for hypo-elastic based elasto-plastic models by Noels *et al.* [12][‡]. In this paper we compare previous results with

(i) The EMCA scheme developed in this paper with the variational formulation of elasto-plastic updates.

(ii) The Newmark [1] scheme combined with the variational formulation of elasto-plastic updates.

We will compare results obtained with the following constant time step sizes: $0.4\mu s$, $0.2\mu s$, $0.1\mu s$, $0.05\mu s$ and $0.025\mu s$.

[Figure 6 about here.]

[Figure 7 about here.]

[Table 3 about here.]

[Figure 8 about here.]

[Figure 9 about here.]

Equivalent plastic strains obtained with the consistent algorithm are illustrated in Figure 6. Let us point out that the model used is a 3-dimension one, but for clarity purpose we represent a slice. For the different time step sizes, results are similar. But with the Newmark scheme it appears that when time step size is larger than $0.05\mu s$ the equivalent strains are

[‡]In [12], nodes belonging to the face $z = 0$ have no initial velocity to be able to verify the balance of the energy. In fact, if these nodes have an initial velocity, the constraints correspond to a modification of the boundary conditions, and therefore the sum of the kinetic energy and the work of internal forces does not remain constant. In the present paper these nodes have an initial velocity, leading to a slightly different result than in [12].

overestimated (Figure 7). When time step size is multiplied by 8, strains are overestimated by about 10%. When analyzing the final results obtained (Table III), it appears that with the EMCA scheme they are similar whatever time step and that they correspond to previous results obtained by Meng and Laursen [9]. But for the Newmark scheme (both present results and those presented by Simo [35]) when the time step increases, the final radius and the maximal equivalent strain are overestimated, while the final length is slightly underestimated. Figure 8(a) illustrates the plastically dissipated energy (initial kinetic energy is equal to $59.57J$). This value is underestimated when the time size increases, mostly for the Newmark scheme. Figure 8(b) illustrates the error on this value. The EMCA scheme is second order accurate with respect to the time step size. Figure 9a illustrates the number of Newton-Raphson iterations. This number is similar for the Newmark scheme and for the consistent algorithm. Cost of evaluation of the internal forces and stiffness matrix for the consistent scheme is twice higher than for the Newmark scheme. The stiffness matrix resulting from the proposed formulation is non-symmetric. But, due to the quasi-incompressible formulation, the volumic part of the stiffness matrix of the traditional Newmark scheme is not symmetric either, and thus this lack of symmetry does not play against the consistent scheme. Overall, the consistent scheme is not more expensive since time step size can be larger to integrate with the same accuracy. Figure 9b illustrates the number of line-search iterations. For the consistent scheme, if time step size increases, this number increases too. For the Newmark scheme this number is almost always lower than for the consistent scheme.

5.3. Numerical example 3: impact of two cylinders

[Figure 10 about here.]

[Table 4 about here.]

Let us now study the impact of two cylinders. Geometry is illustrated in Figure 10 and properties are reported in Table IV. Each cylinder is discretized into 192 quadrangles. The left cylinder has an initial velocity $\dot{\vec{x}}_0$ and impacts the right one initially at rest. Both cylinders are identical and are made of a perfectly plastic material. Frictionless contact is treated with the consistent method proposed by Armero and Petöcz [14]. This example was first proposed by Meng and Laursen [10] in the framework of consistent time algorithm for hyper-elastic based elasto-plastic models, and was also studied by Noels *et al.* [12] in the framework of consistent time algorithm for hypo-elastic based elasto-plastic models. In this paper we compare previous results with

(i) The EMCA scheme developed in this paper with the variational formulation of elasto-plastic updates.
(ii) The Newmark [1] scheme combined with the variational formulation of elasto-plastic updates.

We will compare results obtained with the following constant time step sizes: $20ms$, $10ms$, $5ms$ and $2.5ms$.

[Figure 11 about here.]

[Figure 12 about here.]

[Figure 13 about here.]

[Figure 14 about here.]

When studying the effect of the time step size we have to notice that for the Newmark algorithm both simulations with $\Delta t = 20ms$ and $\Delta t = 10ms$ need a reduction of the step[§] during the contact phase. Figure 11 illustrates the equivalent von Mises stress obtained by the two algorithms with $\Delta t = 2.5ms$. It appears that results are quite similar. But when using a larger time step $\Delta t = 20ms$, if the solution obtained with the EMCA algorithm (Figure 12(a)) remains similar that the one with $\Delta t = 2.5ms$, the solution obtained with Newmark algorithm is quite different (12(b)). If we analyse the time evolution of the energy that is plastically dissipated (Figure 13(a)) with a time step equal to $\Delta t = 20ms$, it appears that the EMCA algorithm gives the same solution than those obtained by Meng and Laursen [10] and with an hypo-elastic model [12]. The Newmark solution diverges after a few ms to reach a 100% error. If we analyse the effect of the time step size (Figure 13(b)) on this plastically dissipated energy, it appears that for the Newmark scheme only the solution obtained with $\Delta t = 2.5ms$ corresponds to the EMCA solutions. The fact that the Newmark algorithm is not designed to integrate a non-linear model (the work of internal forces is different from the sum of the internal energy and the plastically dissipated energy [36]) leads to this error, but there is another problem. If we analyse the time evolution of the work of contact forces (Figure 14(a)) it appears that the Newmark algorithm with $\Delta t = 20ms$ introduces some energy into the system. If we analyse the final results (Figure 14(b)) it appears that for the Newmark scheme the larger the time step size the larger the energy numerically introduced. With the EMCA scheme this energy is always strictly equal to zero.

[§]Tile step size is divided by three when the Newton-Raphson iterative scheme does not converge.

5.4. Numerical example 4: impact of two hollow cylinders

[Figure 15 about here.]

[Table 5 about here.]

[Figure 16 about here.]

[Figure 17 about here.]

The problem under consideration is the interaction of two hollow perpendicular cylinders (Figure 15a). Both cylinders have the same geometry and are both in steel (Table V). The right cylinder has no initial velocity, while the left one has an initial velocity (Table V). Each cylinder has 330 trilinear bricks (1 through the thickness, 22 along the circumference, 15 along the length). The interaction between the cylinders occurs with a Coulomb frictional law. The contact interaction is treated in the consistent way we proposed in [37], based on the method of Armero and Petzöcz [15]. With this formalism, the work of the contact forces is equal to the friction dissipation once the contact is released. The time step used is $\Delta t = 1\mu s$. Figure 15b illustrates the configuration once the contact is released.

Figure 16a illustrates the time evolution of the linear momentum along x for each cylinder. During the contact the left cylinder gives a part of its momentum to the right one. The sum is constant over the time. Figure 16b illustrates the time evolution of the angular momentum along z for each cylinder. Since the impact occurs above the center of gravity of the right cylinder, this generates a rotation of the two cylinders. But after a while the rotation velocity decreases, because of the friction between cylinders. The angular momentum for the two cylinders is constant. Figure 17a illustrates the work of the contact forces. Once the contact is released, this work corresponds to the frictional dissipation (see [37] for details). When

comparing to the initial kinetic energy (Figure 17b), this work is small. Half of the initial kinetic energy is plastically dissipated (Figure 17b) and a small part is transformed into elastic energy. This example illustrates the robustness of the scheme when treating 3D-impact problems.

6. CONCLUSIONS

In this paper we have presented a new formulation of the internal forces for an elasto-plastic material using a variational formulation of visco-plastic updates. This formulation is similar to the one Gonzalez has developed for elasticity, leading to an energy-momentum conserving scheme, but the new formulation presented is able to take into account the plastic behavior. When plasticity occurs, the work of the internal forces corresponds to the sum of the internal energy variation with the energy plastically dissipated energy, leading to a consistent time integration scheme. This property is not verified with a traditional Newmark algorithm. Since the energy is preserved in the non-linear range no numerical energy is introduced in the system during the time integration. This result is very important because it demonstrates that the scheme is numerically stable in the non-linear range. This is a necessary condition for accuracy of the results. Nevertheless, it can be useful to introduce in this scheme numerical dissipation to decrease the oscillations in the answer due to the high frequency numerical modes. The proposed scheme is second order accurate with the time step size and has shown a good accuracy on the numerical examples. The advantage of our formulation is that there is no restriction on the hardening laws, even if in this paper we have used only isotropic hardening.

APPENDIX

I. FORMULATION OF ELASTO-PLASTIC UPDATES FOR BI-LOGARITHMIC POTENTIALS USING THE QUASI-INCOMPRESSIBLE METHOD

Relations (62) implies that $\mathbf{F^{pl}}$ has a determinant equal to the unity. Using relations (42) then leads to

$$J = \det\left(\mathbf{F^{el}}\mathbf{F^{pl}}\right) = \det\mathbf{F^{el}} = J^{\mathrm{el}} \tag{92}$$

Then, using (62), relation (5) becomes

$$\left[\hat{\mathbf{C}}^{\mathbf{el}}\right]^{n+1} = \left[\frac{1}{J^{n+1}}\right]^{\frac{2}{3}} \mathbf{A}^{-T}\left(\Delta\varepsilon^{\mathrm{pl}}\right)\left[\mathbf{F^{pl}}^{n}\right]^{-T}\mathbf{C}^{n+1}\left[\mathbf{F^{pl}}^{n}\right]^{-1}\mathbf{A}^{-1}\left(\Delta\varepsilon^{\mathrm{pl}}\right) \tag{93}$$

This relation allow us to define the elastic predictor

$$\hat{\mathbf{C}}^{\mathbf{pr}} = \left[\frac{1}{J^{n+1}}\right]^{\frac{2}{3}}\left[\mathbf{F^{pl}}^{n}\right]^{-T}\mathbf{C}^{n+1}\left[\mathbf{F^{pl}}^{n}\right]^{-1} \tag{94}$$

Using the split of the potential considered in section 2.3.1, leads to a new expression of the elastic potential

$$\Phi^{\mathrm{el}^{n+1}}\left(\mathbf{C}^{n+1},\mathbf{F^{pl}}^{n+1}\right) = \Phi^{\mathrm{vol}}\left(\det\mathbf{C}^{n+1}\right) + \hat{\Phi}^{\mathrm{el}}\left(\mathbf{A}^{-T}\left(\Delta\varepsilon^{\mathrm{pl}}\right)\hat{\mathbf{C}}^{\mathbf{pr}}\mathbf{A}^{-1}\left(\Delta\varepsilon^{\mathrm{pl}}\right)\right) \tag{95}$$

Assuming pure isotropic hardening is equivalent to choosing the plastic potential

$$\Phi^{\mathrm{pl}^{n+1}} = \Phi^{\mathrm{pl}^{n+1}}\left(\varepsilon^{\mathrm{pl}^{n+1}}\right) \tag{96}$$

with the hardening parameter h and the yield stress Σ_v defined by

$$\Sigma_v = \frac{\partial\Phi^{\mathrm{pl}^{n+1}}\left(\varepsilon^{\mathrm{pl}^{n+1}}\right)}{\partial\varepsilon^{\mathrm{pl}^{n+1}}} \quad \text{and } h = \frac{\partial^2\Phi^{\mathrm{pl}^{n+1}}\left(\varepsilon^{\mathrm{pl}^{n+1}}\right)}{\partial\left[\varepsilon^{\mathrm{pl}^{n+1}}\right]^2} \tag{97}$$

In the particular case of linear hardening, $\Phi^{\mathrm{pl}^{n+1}} = \Sigma_{v0}\varepsilon^{\mathrm{pl}^{n+1}} + \frac{h}{2}\left[\varepsilon^{\mathrm{pl}^{n+1}}\right]^2$ with Σ_{v0} the

initial yield stress. The dissipation dual pseudo potential (50) is then rewritten as

$$\Psi^* = \begin{cases} Y_0 \frac{{\varepsilon^{\rm pl}}^{n+1} - {\varepsilon^{\rm pl}}^n}{\Delta t} & \text{if } {\varepsilon^{\rm pl}}^{n+1} - {\varepsilon^{\rm pl}}^n \geq 0 \\ \infty & \text{if } \dot{\varepsilon^{\rm pl}} < 0 \end{cases} \tag{98}$$

with $Y_0 = 0$ a particular case.

With these definitions, functional (63) can be rewritten as

$$\Delta D\left(\mathbf{F}^{n+1}, \mathbf{F}^n, {\varepsilon^{\rm pl}}^{n+1}, {\varepsilon^{\rm pl}}^n, \mathbf{N}\right) = \Phi^{{\rm pl}^{n+1}} - \Phi^{{\rm pl}^n} + \Phi^{\rm vol}\left(\det\mathbf{C}^{n+1}\right) - \Phi^{\rm vol}\left(\det\mathbf{C}^n\right) + \hat{\Phi}^{\rm el}\left(\mathbf{A}^{-T}\left(\Delta\varepsilon^{\rm pl}\right)\hat{\mathbf{C}}^{\mathbf{pr}}\mathbf{A}^{-1}\left(\Delta\varepsilon^{\rm pl}\right)\right) - \hat{\Phi}^{\rm el}\left(\mathbf{F}^n, {\varepsilon^{\rm pl}}^n\right) + \Delta t\Psi^*\left(\frac{{\varepsilon^{\rm pl}}^{n+1} - {\varepsilon^{\rm pl}}^n}{\Delta t}\right) \tag{99}$$

I.1. Minimisation with respect to ${\varepsilon^{pl}}^{n+1}$.

Functional (99) is derived with respect to ${\varepsilon^{\rm pl}}^{n+1}$. First let us study the differentiation of $\hat{\Phi}^{\rm el}$, that is rewritten in a similar form to that in the elastic case (37). Assuming $\hat{\mathbf{C}}^{\mathbf{pr}}$ and $\mathbf{A}^{-1}$ commute (this will be demonstrated *a posteriori*), and using relations (61) and (62), it leads to

$$\begin{aligned} \hat{\Phi}^{\rm el} &= \frac{G_0}{4}\ln\left(\mathbf{A}^{-T}\left(\Delta\varepsilon^{\rm pl}\right)\hat{\mathbf{C}}^{\mathbf{pr}}\mathbf{A}^{-1}\left(\Delta\varepsilon^{\rm pl}\right)\right) : \ln\left(\mathbf{A}^{-T}\left(\Delta\varepsilon^{\rm pl}\right)\hat{\mathbf{C}}^{\mathbf{pr}}\mathbf{A}^{-1}\left(\Delta\varepsilon^{\rm pl}\right)\right) \\ &= \frac{G_0}{4}\left[\ln\hat{\mathbf{C}}^{\mathbf{pr}} - 2\Delta\varepsilon^{\rm pl}\mathbf{N}\right] : \left[\ln\hat{\mathbf{C}}^{\mathbf{pr}} - 2\Delta\varepsilon^{\rm pl}\mathbf{N}\right] \end{aligned} \tag{100}$$

Deriving this expression with respect to ${\varepsilon^{\rm pl}}^{n+1}$ yields

$$\frac{\partial\hat{\Phi}^{\rm el}}{\partial{\varepsilon^{\rm pl}}^{n+1}} = -G_0\left[\ln\hat{\mathbf{C}}^{\mathbf{pr}} - 2\Delta\varepsilon^{\rm pl}\mathbf{N}\right] : \mathbf{N} \tag{101}$$

Finally the derivative of (99) is obtained by using relations (97), (98) and (101), and leading to

$$G_0\left[\ln\hat{\mathbf{C}}^{\mathbf{pr}} - 2\Delta\varepsilon^{\rm pl}\mathbf{N}\right] : \mathbf{N} = \Sigma_v\left({\varepsilon^{\rm pl}}^{n+1}\right) + Y_0 \tag{102}$$

I.2. Minimization with respect to $\mathbf{N}$.

The functional (99) must be minimum with respect to $\mathbf{N}$ under the constraints (44). Since only $\hat{\Phi}^{\mathrm{el}}$ depends on $\mathbf{N}$, one must have

$$\min_{\mathbf{N},\lambda_1,\lambda_2} \left(\frac{G_0}{4} \left[\ln \hat{\mathbf{C}}^{\mathbf{pr}} - 2\Delta\varepsilon^{\mathrm{pl}}\mathbf{N} \right] : \left[\ln \hat{\mathbf{C}}^{\mathbf{pr}} - 2\Delta\varepsilon^{\mathrm{pl}}\mathbf{N} \right] + \lambda_1 \mathrm{tr}\mathbf{N} + \lambda_2 \left[\mathbf{N} : \mathbf{N} - \frac{3}{2} \right] \right) \tag{103}$$

leading to

$$\mathbf{N} = \frac{\sqrt{\frac{3}{2}} \ln \hat{\mathbf{C}}^{\mathbf{pr}}}{\sqrt{\ln \hat{\mathbf{C}}^{\mathbf{pr}} : \ln \hat{\mathbf{C}}^{\mathbf{pr}}}} \tag{104}$$

Let us note that this last expression ensures that both $\mathbf{A}$ and $\hat{\mathbf{C}}^{\mathbf{pr}}$ have the same spectral basis, and therefore commute.

Combining relations (102) and (104) leads to the equation giving ${\varepsilon^{\mathrm{pl}}}^{n+1}$. Indeed, one has

$$\Sigma_v \left({\varepsilon^{\mathrm{pl}}}^{n+1} \right) + 3G_0 {\varepsilon^{\mathrm{pl}}}^{n+1} = G_0 \sqrt{\frac{3}{2} \ln \hat{\mathbf{C}}^{\mathbf{pr}} : \ln \hat{\mathbf{C}}^{\mathbf{pr}}} + 3G_0 {\varepsilon^{\mathrm{pl}}}^{n} - Y_0 \tag{105}$$

Finally, (104) and (105) allow us to compute $\mathbf{F}^{\mathbf{pl}}$ thanks to (61).

I.3. Stress derivation.

At this point, functional (99) depends only on $\mathbf{F}^{n+1}$, and is rewritten

$$\Delta D_{\mathrm{eff}} \left(\mathbf{C}^{n+1}, \mathbf{C}^{n} \right) = \Phi^{\mathrm{vol}} \left(\det \mathbf{C}^{n+1} \right) - \Phi^{\mathrm{vol}} \left(\det \mathbf{C}^{n} \right) + \widehat{\Delta D}_{\mathrm{eff}} \left(\mathbf{C}^{n+1}, \mathbf{C}^{n} \right) \tag{106}$$

with

$$\begin{aligned} \widehat{\Delta D}_{\mathrm{eff}} \left(\mathbf{C}^{n+1}, \mathbf{C}^{n} \right) = {} & \hat{\Phi}^{\mathrm{el}} \left({\mathbf{F}^{\mathbf{pl}}}^{n+1^{-T}} \hat{\mathbf{C}}^{n+1} {\mathbf{F}^{\mathbf{pl}}}^{n+1^{-1}} \right) + \left[\hat{\Phi}^{\mathrm{pl}} \right]^{n+1} - \\ & \left[\hat{\Phi}^{\mathrm{el}} + \hat{\Phi}^{\mathrm{pl}} \right]^{n} + \Delta t \Psi^{*} \end{aligned} \tag{107}$$

We can also define

$$D_{\mathrm{eff}}^{n+1} \left(\mathbf{C}^{n+1}, \mathbf{C}^{n} \right) = D_{\mathrm{eff}}^{n} + \Delta D_{\mathrm{eff}} \left(\mathbf{C}^{n+1}, \mathbf{C}^{n} \right) \tag{108}$$

Proceeding as in section 2.3.1, second Piola-Kirchhoff stress tensor $\mathbf{PK}$ is obtained by differentiation of (106) with respect to $\mathbf{C}^{n+1}$, and becomes

$$\begin{aligned}\mathbf{PK}^{n+1} &= \frac{\partial \Delta D_{\text{eff}}\left(\mathbf{C}^{n+1},\mathbf{C}^{n}\right)}{\partial \mathbf{C}^{n+1}} \\ &= \underbrace{\frac{\partial \Phi^{\text{vol}}\left(\theta^{e}\right)}{\partial \theta^{e}}}_{p^{e}} J\mathbf{C}^{n+1^{-1}} + 2\frac{\partial \hat{\Phi}^{\text{el}}\left(\hat{\mathbf{C}}^{\mathbf{el}}\right)}{\partial \hat{\mathbf{C}}^{\mathbf{el}}} : \frac{\partial \mathbf{F}^{\mathbf{pl}^{n+1^{-T}}}\hat{\mathbf{C}}^{n+1}\mathbf{F}^{\mathbf{pl}^{n+1^{-1}}}}{\partial \mathbf{C}^{n+1}}\end{aligned} \tag{109}$$

with θ^e computed from (23) and with, the deviatoric part computed by using (41)

$$\frac{\partial \hat{\Phi}^{\text{el}}\left(\hat{\mathbf{C}}^{\mathbf{el}}\right)}{\partial \hat{\mathbf{C}}^{\mathbf{el}}} = \frac{G_0}{2}\sum_{\alpha=1}^{3}\left\{\frac{\ln \lambda^{(\alpha)}}{\lambda^{(\alpha)}}\vec{e}^{(\alpha)}\otimes\vec{e}^{(\alpha)}\right\} \tag{110}$$

In this last expression, we have used the spectral decomposition

$$\hat{\mathbf{C}}^{\mathbf{el}} = \sum_{\alpha=1}^{3}\left\{\lambda^{(\alpha)}\vec{e}^{(\alpha)}\otimes\vec{e}^{(\alpha)}\right\} \tag{111}$$

Moreover, using (36) leads to

$$\frac{\partial \mathbf{F}^{\mathbf{pl}^{n+1^{-T}}}\hat{\mathbf{C}}^{n+1}\mathbf{F}^{\mathbf{pl}^{n+1^{-1}}}}{\partial \mathbf{C}^{n+1}} = \left[\frac{1}{J}\right]^{\frac{2}{3}}\mathbf{f}^{\mathbf{pl}^{n+1^{T}}}\left[\mathcal{I}-\frac{1}{3}\mathbf{C}^{n+1}\otimes\mathbf{C}^{n+1^{-1}}\right]\mathbf{f}^{\mathbf{pl}^{n+1}} \tag{112}$$

and relation (109) is rewritten as

$$\mathbf{PK}^{n+1} = p^{e}J\left[\mathbf{C}^{n+1}\right]^{-1} + \underbrace{2\left[\frac{1}{J}\right]^{\frac{2}{3}}\text{DEV}\left(\mathbf{f}^{\mathbf{pl}^{n+1}}\frac{\partial \hat{\Phi}^{\text{el}}\left(\hat{\mathbf{C}}^{\mathbf{el}}\right)}{\partial \hat{\mathbf{C}}^{\mathbf{el}}}\mathbf{f}^{\mathbf{pl}^{n+1^{T}}}\right)}_{=\frac{\partial \Delta D_{\text{eff}}}{\partial \mathbf{C}}} \tag{113}$$

II. CONSISTENT TANGENT STIFFNESS MATRIX

Let the consistent tangent stiffness matrix $\mathbf{K}$ be defined by

$$\mathbf{K}_{ik}^{\xi\mu} = \frac{\partial \left[\vec{F}_{\text{int}}^{n+\frac{1}{2}}\right]_i^{\xi}}{\partial \left[\vec{x}^{n+1}\right]_k^{\mu}} = \underbrace{\int_{\mathbb{V}_0} \left\{ \frac{\partial \frac{\mathbf{F}_{ir}^{n+1}+\mathbf{F}_{ir}^{n}}{2}}{\partial \left[\vec{x}^{n+1}\right]_k^{\mu}} \left[\mathbf{P}\hat{\mathbf{K}}_{rj}^{n+\frac{1}{2}} + 2p^{n+\frac{1}{2}}\mathbf{dG}_{rj}\right] \vec{D}_j^{\xi} \right\} d\mathbb{V}_0}_{\mathbf{K}_{\mathbf{ik}}^{\mathbf{geo}}} +$$

$$\underbrace{\int_{\mathbb{V}_0} \left\{ \frac{\mathbf{F}_{ir}^{n+1}+\mathbf{F}_{ir}^{n}}{2} \frac{\partial \mathbf{P}\hat{\mathbf{K}}_{rj}^{n+\frac{1}{2}}}{\partial \left[\vec{x}^{n+1}\right]_k^{\mu}} \vec{D}_j^{\xi} \right\} d\mathbb{V}_0}_{\mathbf{K}_{\mathbf{ik}}^{\mathbf{dev}}} + \underbrace{\int_{\mathbb{V}_0} \left\{ \frac{\mathbf{F}_{ir}^{n+1}+\mathbf{F}_{ir}^{n}}{2} \frac{\partial 2p^{n+\frac{1}{2}}\mathbf{dG}_{rj}}{\partial \left[\vec{x}^{n+1}\right]_k^{\mu}} \vec{D}_j^{\xi} \right\} d\mathbb{V}_0}_{\mathbf{K}_{\mathbf{ik}}^{\mathbf{vol}}} \tag{114}$$

Let us use the following results

$$\frac{\partial \mathbf{F}_{ij}^{n+1}}{\partial \left[\vec{x}^{n+1}\right]_k^{\mu}} = \vec{D}_j^{\mu}\delta_{ik} \quad \text{and} \quad \frac{\partial \mathbf{C}_{ij}^{n+1}}{\partial \vec{x}_k^{\mu}} = \left[\delta_{li}\mathbf{F}_{kj}^{n+1} + \mathbf{F}_{ki}^{n+1}\delta_{lj}\right] \vec{D}_l^{\mu} \tag{115}$$

and

$$\frac{\partial \left\|\mathbf{C}^{n+1} - \mathbf{C}^{n}\right\|^2}{\partial \mathbf{C}^{n+1}} = 2\mathbf{C}^{n+1} - 2\mathbf{C}^{n} \quad \text{and} \quad \frac{\partial \sqrt{\det \mathbf{C}^{n+1}}}{\partial \mathbf{C}^{n+1}} = \frac{1}{2}\sqrt{\det \mathbf{C}^{n+1}}\mathbf{C}^{n+1-T} \tag{116}$$

II.1. Geometrical part

Using relations (115), the geometrical part from relation (114) can be computed as

$$\begin{aligned} \mathbf{K}^{\mathbf{geo}\,\xi\mu}_{ik} &= \int_{\mathbb{V}_0} \left\{ \frac{\partial \frac{\mathbf{F}_{ir}^{n+1}+\mathbf{F}_{ir}^{n}}{2}}{\partial \left[\vec{x}^{n+1}\right]_k^{\mu}} \left[\mathbf{P}\hat{\mathbf{K}}_{rj}^{n+\frac{1}{2}} + 2p^{n+\frac{1}{2}}\mathbf{dG}_{rj}\right] \vec{D}_j^{\xi} \right\} d\mathbb{V}_0 \\ &= \int_{\mathbb{V}_0} \left\{ \vec{D}_j^{\xi} \mathcal{G}_{ijkl} \vec{D}_l^{\xi} \right\} d\mathbb{V}_0 \end{aligned} \tag{117}$$

with the four order tensor $\mathcal{G}$ defined by

$$\mathcal{G}_{ijkl} = \frac{1}{2}\delta_{ik}\left[\mathbf{P}\hat{\mathbf{K}}_{lj}^{n+\frac{1}{2}} + 2p^{n+\frac{1}{2}}\mathbf{dG}_{lj}\right] \tag{118}$$

II.2. Volumic part

The volumic part is decomposed into two terms. The first one results from the differentiation of the constant pressure (over the element), while the second one results from the differentiation of $\mathbf{dG}$.

Using (23), the first term becomes

$$\begin{aligned}\mathbf{K}^{\mathrm{vol1}\,\xi\mu}_{ik} &= \int_{\mathbb{V}_0}\left\{\frac{\mathbf{F}^{n+1}_{ir}+\mathbf{F}^{n}_{ir}}{2}\mathbf{dG}_{rj}\vec{D}^{\xi}_{j}\frac{\partial 2p^{n+\frac{1}{2}}}{\partial\theta^{e\,n+1}}\frac{\partial\theta^{e\,n+1}}{\partial\vec{x}^{\mu}_{k}}\right\}d\mathbb{V}_0 \\ &= \int_{\mathbb{V}_0}\left\{\vec{D}^{\xi}_{j}\mathcal{H}^{\mathrm{vol1}}_{ijkl}\frac{1}{\mathbb{V}_0}\int_{\mathbb{V}_0}\left\{J\mathbf{f}^{n+1\,T}_{lp}\vec{D}^{\mu}_{p}\right\}d\mathbb{V}_0\right\}d\mathbb{V}_0 \end{aligned} \tag{119}$$

with (using (82))

$$\begin{aligned}\mathcal{H}^{\mathrm{vol1}}_{ijkl} = & \quad \frac{\mathbf{F}^{n+1}_{ir}+\mathbf{F}^{n}_{ir}}{2}\mathbf{dG}_{rj}\delta_{kl}\frac{\partial^2\Phi^{\mathrm{vol}}}{\partial\theta^{e\,2}}\left(\frac{\theta^{e\,n+1}+\theta^{e\,n}}{2}\right) && \text{if } \theta^{e\,n+1}=\theta^{e\,n} \\ = & \quad \frac{\mathbf{F}^{n+1}_{ir}+\mathbf{F}^{n}_{ir}}{2}\mathbf{dG}_{rj}\delta_{kl}2\left[\frac{\frac{\partial\Phi^{\mathrm{vol}}}{\partial\theta^{e}}\left(\theta^{e\,n+1}\right)-\frac{\Phi^{\mathrm{vol}}\left(\theta^{e\,n+1}\right)-\Phi^{\mathrm{vol}}\left(\theta^{e\,n}\right)}{\Delta\theta^{e}}}{\Delta\theta^{e}}\right] && \text{if } \theta^{e\,n+1}\neq\theta^{e\,n}\end{aligned} \tag{120}$$

The second term becomes

$$\mathbf{K}^{\mathrm{vol2}\,\xi\mu}_{ik} = \int_{\mathbb{V}_0}\left\{\frac{\mathbf{F}^{n+1}_{ir}+\mathbf{F}^{n}_{ir}}{2}2p^{n+\frac{1}{2}}\frac{\partial\mathbf{dG}_{rj}}{\partial\left[\vec{x}^{n+1}\right]^{\mu}_{k}}\vec{D}^{\xi}_{j}\right\}d\mathbb{V}_0 = \int_{\mathbb{V}_0}\left\{\vec{D}^{\xi}_{j}\mathcal{H}^{\mathrm{vol2}}_{ijkl}\vec{D}^{\mu}_{l}\right\} \tag{121}$$

where (using (115), and the symmetry properties of $\mathbf{C}$)

$$\begin{aligned}\mathcal{H}^{\mathrm{vol2}}_{ijkl} &= 2p^{n+\frac{1}{2}}\frac{\mathbf{F}^{n+1}_{ir}+\mathbf{F}^{n}_{ir}}{2}\frac{\partial\mathbf{dG}_{rj}}{\partial\mathbf{C}^{n+1}_{mn}}\left[\delta_{ml}\mathbf{F}^{n+1\,T}_{nk}+\mathbf{F}^{n+1\,T}_{mk}\delta_{nl}\right] \\ &= 4p^{n+\frac{1}{2}}\frac{\mathbf{F}^{n+1}_{ir}+\mathbf{F}^{n}_{ir}}{2}\mathbf{F}^{n+1}_{km}\frac{\partial\mathbf{dG}_{rj}}{\partial\mathbf{C}^{n+1}_{ml}}\end{aligned} \tag{122}$$

Using relations (81) and (116), one has

$$\begin{aligned}\frac{\partial\mathbf{dG}}{\partial\mathbf{C}^{n+1}} &= \frac{1}{2}\left[\mathcal{I}-\frac{\boldsymbol{\Delta}\mathbf{C}\otimes\boldsymbol{\Delta}\mathbf{C}}{\|\boldsymbol{\Delta}\mathbf{C}\|^2}\right]:\frac{\partial\mathbf{DG}^{n+\frac{1}{2}}}{\partial\mathbf{C}^{n+\frac{1}{2}}}-\frac{\boldsymbol{\Delta}\mathbf{C}\otimes\mathbf{DG}^{n+\frac{1}{2}}}{\|\boldsymbol{\Delta}\mathbf{C}\|^2}+\frac{1}{2}J^{n+1}\frac{\boldsymbol{\Delta}\mathbf{C}\otimes\mathbf{C}^{n+1\,-1}}{\|\boldsymbol{\Delta}\mathbf{C}\|^2} \\ &+\left[\frac{J^{n+1}-J^{n}-\mathbf{DG}^{n+\frac{1}{2}}:\boldsymbol{\Delta}\mathbf{C}}{\|\boldsymbol{\Delta}\mathbf{C}\|^2}\right]\left[\mathcal{I}-2\frac{\boldsymbol{\Delta}\mathbf{C}\otimes\boldsymbol{\Delta}\mathbf{C}}{\|\boldsymbol{\Delta}\mathbf{C}\|^2}\right]\end{aligned} \tag{123}$$

with

$$\frac{\partial\mathbf{DG}^{n+\frac{1}{2}}}{\partial\mathbf{C}^{n+\frac{1}{2}}} = \frac{1}{2}\sqrt{\det\left(\mathbf{C}^{n+\frac{1}{2}}\right)}\left[\frac{1}{2}\mathbf{C}^{n+\frac{1}{2}\,-1}\otimes\mathbf{C}^{n+\frac{1}{2}\,-1}-\mathcal{I}_{\mathbf{C}^{n+\frac{1}{2}\,-1}}\right] \tag{124}$$

In this expression we use the notations $\mathbf{C}^{n+\frac{1}{2}} = \frac{\mathbf{C}^{n+1}+\mathbf{C}^n}{2}$ and $[\mathcal{I}_{\mathbf{A}}]_{ijkl} = \frac{1}{2}\mathbf{A}_{ik}\mathbf{A}_{jl} + \frac{1}{2}\mathbf{A}_{il}\mathbf{A}_{jk}$.

II.3. Deviatoric part

Using relations (115), the deviatoric term becomes

$$\mathbf{K}^{\mathrm{dev}}{}^{\xi\mu}_{ik} = \int_{\mathbb{V}_0} \left\{ \frac{\mathbf{F}^{n+1}_{ir} + \mathbf{F}^{n}_{ir}}{2} \frac{\partial \hat{\mathbf{PK}}^{n+\frac{1}{2}}_{rj}}{\partial \left[\vec{x}^{n+1}\right]^{\mu}_{k}} \vec{D}^{\xi}_{j} \right\} d\mathbb{V}_0 = \int_{\mathbb{V}_0} \left\{ \vec{D}^{\xi}_{j} \mathcal{H}^{\mathrm{dev}}_{ijkl} \vec{D}^{\mu}_{l} \right\} d\mathbb{V}_0 \qquad (125)$$

with

$$\mathcal{H}^{\mathrm{dev}}_{ijkl} = \frac{\mathbf{F}^{n+1}_{ir} + \mathbf{F}^{n}_{ir}}{2} \mathbf{F}^{n+1}_{km} 2 \frac{\partial \hat{\mathbf{PK}}^{n+\frac{1}{2}}_{rj}}{\mathbf{C}^{n+1}_{ml}} \qquad (126)$$

Using relations (83) and (116) yields

$$\begin{aligned} 2\frac{\partial \hat{\mathbf{PK}}^{n+\frac{1}{2}}}{\mathbf{C}^{n+1}} = {} & \frac{1}{2}\left[\mathcal{I} - \frac{\boldsymbol{\Delta}\mathbf{C}\otimes\boldsymbol{\Delta}\mathbf{C}}{\|\boldsymbol{\Delta}\mathbf{C}\|^2}\right] : \frac{d4\mathbf{D}\widehat{\boldsymbol{\Delta}\mathbf{D}}_{\mathrm{eff}}{}^{n+\frac{1}{2}}}{d\mathbf{C}^{n+\frac{1}{2}}} + \\ & \frac{\boldsymbol{\Delta}\mathbf{C}}{\|\boldsymbol{\Delta}\mathbf{C}\|^2} \otimes 4\frac{d\widehat{\Delta D}_{\mathrm{eff}}\left(\mathbf{C}^{n+1}-\mathbf{C}^{n}\right)}{d\mathbf{C}^{n+1}} - \frac{\boldsymbol{\Delta}\mathbf{C}}{\|\boldsymbol{\Delta}\mathbf{C}\|^2} \otimes 4\mathbf{D}\widehat{\boldsymbol{\Delta}\mathbf{D}}_{\mathrm{eff}}{}^{n+\frac{1}{2}} + \\ & 4\left[\frac{\widehat{\Delta D}_{\mathrm{eff}}\left(\mathbf{C}^{n+1}-\mathbf{C}^{n}\right) - \mathbf{D}\widehat{\boldsymbol{\Delta}\mathbf{D}}_{\mathrm{eff}}{}^{n+\frac{1}{2}} : \boldsymbol{\Delta}\mathbf{C}}{\|\boldsymbol{\Delta}\mathbf{C}\|^2}\right]\left[\mathcal{I} - 2\frac{\boldsymbol{\Delta}\mathbf{C}\otimes\boldsymbol{\Delta}\mathbf{C}}{\|\boldsymbol{\Delta}\mathbf{C}\|^2}\right] \end{aligned} \qquad (127)$$

In this expression, we use differentiation with symbol d and not ∂ because the minimum value of $\Delta\hat{D}$ depends only on $\mathbf{C}$. Moreover, we use exponent $n+\frac{1}{2}$ to refer to values computed for $\frac{\mathbf{C}^{n+1}+\mathbf{C}^n}{2}$.

Let $\mathcal{M} = 4\frac{d\mathbf{D}\widehat{\boldsymbol{\Delta}\mathbf{D}}_{\mathrm{eff}}{}^{n+\frac{1}{2}}}{d\mathbf{C}^{n+\frac{1}{2}}}$ be the material tensor. Proceeding as Simo and Taylor [27] yields

$$\begin{aligned} \mathcal{M} = {} & \det\left(\mathbf{C}^{n+\frac{1}{2}}\right)^{-\frac{2}{3}} \left[\mathcal{C}^{n+\frac{1}{2}} + \frac{4}{3}\left[\mathbf{f}^{\mathbf{pl}}\frac{\partial\hat{\Phi}^{\mathrm{el}}}{\partial\hat{\mathbf{C}}^{\mathbf{el}}}\mathbf{f}^{\mathbf{pl}T} : \hat{\mathbf{C}}\right]^{n+\frac{1}{2}} \left[\mathcal{I}_{\hat{\mathbf{C}}^{-1}} - \frac{1}{3}\hat{\mathbf{C}}^{-1}\otimes\hat{\mathbf{C}}^{-1}\right]^{n+\frac{1}{2}} \right. \\ & \left. -\frac{2}{3}\left[\hat{\mathbf{C}}^{-1}\otimes 2\mathbf{D}\widehat{\boldsymbol{\Delta}\mathbf{D}}_{\mathrm{eff}} + 2\mathbf{D}\widehat{\boldsymbol{\Delta}\mathbf{D}}_{\mathrm{eff}}\otimes\hat{\mathbf{C}}^{-1}\right]^{n+\frac{1}{2}}\right] \end{aligned} \qquad (128)$$

with

$$\begin{aligned} \mathcal{C} = {} & 4\frac{d\mathbf{D}\widehat{\boldsymbol{\Delta}\mathbf{D}}_{\mathrm{eff}}}{d\hat{\mathbf{C}}} - \frac{4}{3}\hat{\mathbf{C}}^{-1}\otimes\left[\hat{\mathbf{C}} : \frac{d\mathbf{D}\widehat{\boldsymbol{\Delta}\mathbf{D}}_{\mathrm{eff}}}{d\hat{\mathbf{C}}}\right] - \frac{4}{3}\left[\frac{d\mathbf{D}\widehat{\boldsymbol{\Delta}\mathbf{D}}_{\mathrm{eff}}}{d\hat{\mathbf{C}}} : \hat{\mathbf{C}}\right]\otimes\hat{\mathbf{C}}^{-1} + \\ & \frac{4}{9}\left[\hat{\mathbf{C}} : \frac{d\mathbf{D}\widehat{\boldsymbol{\Delta}\mathbf{D}}_{\mathrm{eff}}}{d\hat{\mathbf{C}}} : \hat{\mathbf{C}}\right]\hat{\mathbf{C}}^{-1}\otimes\hat{\mathbf{C}}^{-1} \end{aligned} \qquad (129)$$

Now we have to compute $\frac{d\widehat{\Delta D}_{\rm eff}}{d\mathbf{C}^{n+1}}$ and $\frac{d\widehat{\mathbf{D}\boldsymbol{\Delta}\mathbf{D}}_{\rm eff}}{d\hat{\mathbf{C}}}$. First term is obtained by

$$\frac{d\widehat{\Delta D}_{\rm eff}}{d\mathbf{C}^{n+1}} = \frac{d\widehat{\Delta D}_{\rm eff}}{d\hat{\mathbf{C}}^{n+1}} : \frac{\partial \hat{\mathbf{C}}^{n+1}}{\partial \mathbf{C}^{n+1}} = J^{n+1-\frac{2}{3}} \left[{\rm DEV} \frac{d\widehat{\Delta D}_{\rm eff}}{d\hat{\mathbf{C}}^{n+1}} \right]^{n+1} \tag{130}$$

with

$$\frac{d\widehat{\Delta D}_{\rm eff}}{d\hat{\mathbf{C}}^{n+1}} = \frac{\partial \widehat{\Delta D}}{\partial \hat{\mathbf{C}}^{n+1}} + \frac{\partial \widehat{\Delta D}}{\partial {\varepsilon^{\rm pl}}^{n+1}} \frac{\partial {\varepsilon^{\rm pl}}^{n+1}}{\partial \hat{\mathbf{C}}^{n+1}} + \frac{\partial \widehat{\Delta D}}{\partial \mathbf{N}^{n+1}} : \frac{\partial \mathbf{N}^{n+1}}{\partial \hat{\mathbf{C}}^{n+1}} \tag{131}$$

Second term is obtained by

$$\begin{aligned} \left[\frac{d\widehat{\mathbf{D}\boldsymbol{\Delta}\mathbf{D}}_{\rm eff}}{d\hat{\mathbf{C}}} \right]^{n+\frac{1}{2}} = & \left[\frac{\partial \mathbf{D}\boldsymbol{\Delta}\hat{\mathbf{D}}}{\partial \hat{\mathbf{C}}} + \frac{1}{2} \frac{\partial \mathbf{D}\boldsymbol{\Delta}\hat{\mathbf{D}}}{\partial \varepsilon^{\rm pl}} \otimes \frac{\partial \varepsilon^{\rm pl}}{\partial \hat{\mathbf{C}}} + \frac{1}{2} \frac{\partial \varepsilon^{\rm pl}}{\partial \hat{\mathbf{C}}} \otimes \frac{\partial \mathbf{D}\boldsymbol{\Delta}\hat{\mathbf{D}}}{\partial \varepsilon^{\rm pl}} + \right. \\ & \left. \frac{1}{2} \frac{\partial \mathbf{D}\boldsymbol{\Delta}\hat{\mathbf{D}}}{\partial \mathbf{N}} : \frac{\partial \mathbf{N}}{\partial \hat{\mathbf{C}}} + \frac{1}{2} \left[\frac{\partial \mathbf{N}}{\partial \hat{\mathbf{C}}} \right]^{TT} : \left[\frac{\partial \mathbf{D}\boldsymbol{\Delta}\hat{\mathbf{D}}}{\partial \mathbf{N}} \right]^{TT} \right]^{n+\frac{1}{2}} \end{aligned} \tag{132}$$

where ${\mathcal{H}_{ijkl}}^{TT} = \mathcal{H}_{klij}$. In this last expression, we have ensured that $\left[\frac{d\widehat{\mathbf{D}\boldsymbol{\Delta}\mathbf{D}}_{\rm eff}}{d\hat{\mathbf{C}}}\right]_{ijkl} = \left[\frac{d\widehat{\mathbf{D}\boldsymbol{\Delta}\mathbf{D}}_{\rm eff}}{d\hat{\mathbf{C}}}\right]_{klij}$ (to be consistent with the fact that a double differentiation with respect to $\mathbf{C}$ must lead to a symmetric tensor).

II.4. Particular case of bi-logarithmic potential and isotropic hardening

In this section, expressions are valid in configuration $n+1$ and in configuration $n+\frac{1}{2}$. For the volumic part (120), one has easily

$$\frac{\partial^2 \hat{\Phi}^{\rm vol}}{\partial \theta^e \partial \theta^e} = K_0 \frac{1 - \ln(\theta^e)}{{\theta^e}^2} \tag{133}$$

For the deviatoric parts (131) and (132), we have more relations to evaluate. Since only $\hat{\Phi}^{\rm el}$ depends explicitly on $\hat{\mathbf{C}}$, one has

$$\frac{\partial \widehat{\Delta D}}{\partial \hat{\mathbf{C}}} = \frac{\partial \hat{\Phi}^{\rm el}}{\partial \hat{\mathbf{C}}} = \mathbf{f}^{\mathbf{pl}} \frac{\partial \hat{\Phi}^{\rm el}}{\partial \hat{\mathbf{C}}^{el}} {\mathbf{f}^{\mathbf{pl}}}^T \tag{134}$$

with $\frac{\partial \hat{\Phi}^{\rm el}}{\partial \hat{\mathbf{C}}^{el}}$ computed thanks to spectral decomposition.

Since $\widehat{\Delta D}$ is minimum with respect to $\varepsilon^{\rm pl}$, one has

$$\frac{\partial \widehat{\Delta D}}{\partial \varepsilon^{\rm pl}} = 0 \tag{135}$$

Using relation (62) yields

$$\frac{\partial \mathbf{f^{pl}}_{ij}}{\partial \varepsilon^{\mathrm{pl}}} = -\mathbf{f^{pl}}_{im}\mathbf{N}_{mj} \quad \text{and} \quad \frac{\partial \mathbf{f^{pl}}_{ij}}{\partial \mathbf{N}_{kl}} = -\mathbf{f^{pl}}_{im}\mathcal{D}^{\exp}_{mrkl}\mathbf{F^{pl}}^{n}_{rn}\mathbf{f^{pl}}_{nj} \tag{136}$$

where $\mathcal{D}^{\exp} = \frac{\partial \exp\left(\Delta\varepsilon^{\mathrm{pl}}\mathbf{N}\right)}{\partial \mathbf{N}}$ and where $\mathbf{F^{pl}}^{n}$ is the plastic deformation tensor at previous step. Let us define the following operation $[\mathbf{A}\mathcal{H}\mathbf{B}]_{ijkl} = \mathbf{A}_{im}\mathcal{H}_{mnkl}\mathbf{B}_{jn}$, $[\mathcal{H}\mathbf{B}]_{ijkl} = \mathcal{H}_{inkl}\mathbf{B}_{jn}$ and $[\mathbf{A}\mathcal{H}]_{ijkl} = \mathbf{A}_{im}\mathcal{H}_{mjkl}$. Let us define $\mathcal{H}^{T}_{ijkl} = \mathcal{H}_{jilk}$, therefore, using (136) leads to

$$\frac{\partial \widehat{\Delta D}}{\partial \mathbf{N}} = -\left[\mathbf{f^{pl}}\frac{\partial \hat{\Phi}^{\mathrm{el}}}{\partial \hat{\mathbf{C}}^{\mathbf{el}}}\mathbf{f^{pl}}^{T}\right] : \left[\hat{\mathbf{C}}\mathbf{f^{pl}}\mathcal{D}^{\exp}\mathbf{F^{pl}}^{nT}\right] - \left[\mathbf{f^{pl}}\frac{\partial \hat{\Phi}^{\mathrm{el}}}{\partial \hat{\mathbf{C}}^{\mathbf{el}}}\mathbf{f^{pl}}^{T}\right] : \left[\hat{\mathbf{C}}\mathbf{f^{pl}}\mathcal{D}^{\exp}\mathbf{F^{pl}}^{nT}\right]^{T} \tag{137}$$

that is different from zero since minimum of $\widehat{\Delta D}$ is reached under constraints.

From relation (94), one gets

$$\frac{\partial \hat{\mathbf{C}}^{\mathbf{pr}}}{\partial \hat{\mathbf{C}}} = \mathcal{I}_{[\mathbf{f^{pl}}^{n}]^{T}} \tag{138}$$

Therefore, thanks to relation (105), one has

$$\frac{\partial \varepsilon^{\mathrm{pl}^{n+1}}}{\partial \hat{\mathbf{C}}} = \sqrt{\frac{3}{2}}\frac{G_0}{[3G_0+h]\sqrt{\ln \hat{\mathbf{C}}^{\mathbf{pr}} : \ln \hat{\mathbf{C}}^{\mathbf{pr}}}}\ln \hat{\mathbf{C}}^{\mathbf{pr}} : \mathcal{D}^{\ln \hat{\mathbf{C}}^{\mathbf{pr}}} : \mathcal{I}_{[\mathbf{f^{pl}}^{n}]^{T}} \tag{139}$$

with $\mathcal{D}^{\ln \hat{\mathbf{C}}^{\mathbf{pr}}} = \frac{\partial \ln \hat{C}^{pr}}{\partial \hat{\mathbf{C}}}$. Moreover, using relation (104) leads to

$$\begin{aligned}\frac{\partial \mathbf{N}}{\partial \hat{\mathbf{C}}} = {} & \frac{\sqrt{\frac{3}{2}}}{\sqrt{\ln \hat{\mathbf{C}}^{\mathbf{pr}} : \ln \hat{\mathbf{C}}^{\mathbf{pr}}}}\mathcal{D}^{\ln \hat{\mathbf{C}}^{\mathbf{pr}}} : \mathcal{I}_{[\mathbf{f^{pl}}^{n}]^{T}} - \\ & \frac{\sqrt{\frac{3}{2}}\ln \hat{\mathbf{C}}^{\mathbf{pr}}}{\left[\ln \hat{\mathbf{C}}^{\mathbf{pr}} : \ln \hat{\mathbf{C}}^{\mathbf{pr}}\right]^{\frac{3}{2}}} \otimes \ln \hat{\mathbf{C}}^{\mathbf{pr}} : \mathcal{D}^{\ln \hat{\mathbf{C}}^{\mathbf{pr}}} : \mathcal{I}_{[\mathbf{f^{pl}}^{n}]^{T}}\end{aligned} \tag{140}$$

Finally, let us study the missing terms in (132). Let us define the following operation $[\mathbf{AB}\mathcal{H}\mathbf{CD}]_{ijkl} = \mathbf{A}_{im}\mathbf{B}_{jn}\mathcal{H}_{mnpq}\mathbf{C}_{kp}\mathbf{D}_{lq}$, then we have directly

$$\frac{\partial \mathbf{D}\boldsymbol{\Delta}\hat{\mathbf{D}}}{\partial \hat{\mathbf{C}}} = \mathbf{f^{pl}}\mathbf{f^{pl}}\frac{\partial^2 \hat{\Psi}^{\mathrm{el}}}{\partial \hat{\mathbf{C}}^{\mathbf{el}}\partial \hat{\mathbf{C}}^{\mathbf{el}}}\mathbf{f^{pl}}\mathbf{f^{pl}} \tag{141}$$

Using previous definitions and results leads to

$$\begin{aligned}\frac{\partial \mathbf{D}\boldsymbol{\Delta}\hat{\mathbf{D}}}{\partial \varepsilon^{\mathrm{pl}}} &= -\left[\mathbf{f}^{\mathbf{pl}}\mathbf{N}\mathbf{F}^{\mathbf{pl}}\right]\left[\mathbf{f}^{\mathbf{pl}}\frac{\partial \hat{\Psi}^{\mathrm{el}}\left(\hat{\mathbf{C}}^{\mathbf{el}}\right)}{\partial \hat{\mathbf{C}}^{\mathbf{el}}}\mathbf{f}^{\mathbf{pl}^T}\right] - \left[\mathbf{f}^{\mathbf{pl}}\frac{\partial \hat{\Psi}^{\mathrm{el}}\left(\hat{\mathbf{C}}^{\mathbf{el}}\right)}{\partial \hat{\mathbf{C}}^{\mathbf{el}}}\mathbf{f}^{\mathbf{pl}^T}\right]\left[\mathbf{f}^{\mathbf{pl}}\mathbf{N}\mathbf{F}^{\mathbf{pl}}\right]^T \\ &\quad -\frac{\partial \mathbf{D}\boldsymbol{\Delta}\hat{\mathbf{D}}}{\partial \hat{\mathbf{C}}} : \left[\hat{\mathbf{C}}\mathbf{f}^{\mathbf{pl}}\mathbf{N}\mathbf{F}^{\mathbf{pl}}\right] - \frac{\partial \mathbf{D}\boldsymbol{\Delta}\hat{\mathbf{D}}}{\partial \hat{\mathbf{C}}} : \left[\hat{\mathbf{C}}\mathbf{f}^{\mathbf{pl}}\mathbf{N}\mathbf{F}^{\mathbf{pl}}\right]^T \end{aligned} \tag{142}$$

and to

$$\begin{aligned}\frac{\partial \mathbf{D}\boldsymbol{\Delta}\hat{\mathbf{D}}}{\partial \mathbf{N}} &= -\left[\mathbf{f}^{\mathbf{pl}}\mathcal{D}^{\exp}\mathbf{F}^{\mathbf{pl}^{nT}}\right]\left[\mathbf{f}^{\mathbf{pl}}\frac{\partial \hat{\Psi}^{\mathrm{el}}\left(\hat{\mathbf{C}}^{\mathbf{el}}\right)}{\partial \hat{\mathbf{C}}^{\mathbf{el}}}\mathbf{f}^{\mathbf{pl}^T}\right] - \\ &\quad \left[\mathbf{f}^{\mathbf{pl}}\frac{\partial \hat{\Psi}^{\mathrm{el}}\left(\hat{\mathbf{C}}^{\mathbf{el}}\right)}{\partial \hat{\mathbf{C}}^{\mathbf{el}}}\mathbf{f}^{\mathbf{pl}^T}\right]\left[\mathbf{f}^{\mathbf{pl}}\mathcal{D}^{\exp}\mathbf{F}^{\mathbf{pl}^{nT}}\right]^T - \\ &\quad \frac{\partial \mathbf{D}\boldsymbol{\Delta}\hat{\mathbf{D}}}{\partial \hat{\mathbf{C}}} : \left[\hat{\mathbf{C}}\mathbf{f}^{\mathbf{pl}}\mathcal{D}^{\exp}\mathbf{F}^{\mathbf{pl}^{nT}}\right] - \frac{\partial \mathbf{D}\boldsymbol{\Delta}\hat{\mathbf{D}}}{\partial \hat{\mathbf{C}}} : \left[\hat{\mathbf{C}}\mathbf{f}^{\mathbf{pl}}\mathcal{D}^{\exp}\mathbf{F}^{\mathbf{pl}^{nT}}\right]^T \end{aligned} \tag{143}$$

REFERENCES

1. Newmark N. A method of computation for structural dynamics. *Journal of the Engineering Mechanics Division ASCE* 1959; **85**(EM3):67–94.
2. Belytschko T and Schoeberle DF. On the unconditional stability of an implicit algorithm for non-linear structural dynamics. *Journal of Applied Mechanics* 1975; **42**:865–869.
3. Hughes TJR. A note on the stability of Newmark's algorithm in nonlinear structural dynamics. *International Journal of Numerical Methods in Engineering* 1977; **11**(2):383–386.
4. Chung J and Hulbert GJM. A time integration algorithms for structural dynamics with improved numerical dissipations: the generalized-α method. *Journal of Applied Mechanics* 1993; **60**:371–375.
5. Erlicher S, Bonaventura L, and Bursi OS. The analysis of the α-generalized method for non-linear dynamic problems. *Computational Mechanics* 2002; **28**:83–104.
6. Simo JC and Tarnow N. The discrete energy-momentum method. Conserving algorithms for nonlinear elastodynamics. *ZAMP* 1992; **43**:757–792.
7. Laursen TA and Meng X. A new solution procedure for application of energy-conserving algorithms to general constitutive models in nonlinear elastodynamics. *Computer Methods in Applied Mechanics and Engineering* 2001; **190**:6309–6322.

8. Gonzalez O. Exact energy and momentum conserving algorithms for general models in nonlinear elasticity. *Computer Methods in Applied Mechanics and Engineering* 2000; **190**:1763–1783.
9. Meng X and Laursen T. Energy consistent algorithms for dynamic finite deformation plasticity. *Computer Methods in Applied Mechanics and Engineering* 2001; **191**:1639–1675.
10. Meng X and Laursen TA. On energy consistency of large deformation plasticity models, with application to the design of unconditionally stable time integrators. *Finite Elements in Analysis and Design* 2002; **38**:949–963.
11. Noels L, Stainier L, and Ponthot J-P. Energy-momentum conserving algorithm for non-linear hypoelastic constitutive models. *International Journal of Numerical Methods in Engineering* 2004; **59**:83–114.
12. Noels L, Stainier L, and Ponthot J-P. On the use of large time steps with an energy-momentum conserving algorithm for non-linear hypoelastic constitutive models. *International Journal of Solids and Structures* 2004; **41**:663–693.
13. Sansour C, Wriggers P, and Sansour J. On the design of energy-momentum integration schemes for arbitrary continuum formulations. Applications to classical and chaotic motion of shells. *International Journal of Numerical Methods in Engineering* 2004; **60**:2419–2440.
14. Armero F and Petöcz E. Formulation and analysis of conserving algorithms for frictionless dynamic contact/impact problems. *Computer Methods in Applied Mechanics and Engineering* 1998; **158**:269–300.
15. Armero F and Petöcz E. A new dissipative time-stepping algorithm for frictional contact problems: formulation and analysis. *Computer Methods in Applied Mechanics and Engineering* 1999; **179**:151–178.
16. Laursen TA and Chawla V. Design of energy conserving algorithms for frictionless dynamic contact problems. *International Journal of Numerical Methods in Engineering* 1997; **40**:863–886.
17. Chawla V and Laursen T. Energy consistent algorithms for frictional contact problems. *International Journal of Numerical Methods in Engineering* 1998; **42**:799–827.
18. Armero F and Romero I. On the formulation of high-frequency dissipative time-stepping algorithms for non-linear dynamics. Part I: low-order methods for two model problems and nonlinear elastodynamics. *Computer Methods in Applied Mechanics and Engineering* 2001; **190**:2603–2649.
19. Armero F and Romero I. On the formulation of high-frequency dissipative time-stepping algorithms for non-linear dynamics. Part II: second-order methods. *Computer Methods in Applied Mechanics and Engineering* 2001; **190**:6783–6824.
20. Noels L, Stainier L, and Ponthot J-P. Simulation of complex impact problems with implicit time algorithm. Application to a blade-loss problem. *International Journal of Impact Engineering.* Accepted

for publication.

21. Betsch P and Steinmann P. Conservation properties of a time fe method. part i: Time-stepping schemes for n-body problems. *International Journal of Numerical Methods in Engineering* 2000; **49**:599–638.
22. Betsch P and Steinmann P. Conservation properties of a time FE method. part II: Time-stepping schemes for non-linear elastodynamics. *International Journal of Numerical Methods in Engineering* 2001; **50**:1931–1955.
23. Bauchau OA and Joo T. Computational schemes for non-linear elasto-dynamics. *International Journal of Numerical Methods in Engineering* 1999; **45**:693–719.
24. Bottasso CL and Borri M. Integrating finite rotation. *Computer Methods in Applied Mechanics and Engineering* 1998; **164**:307–331.
25. Ortiz M and Stainier L. The variational formulation of viscoplastic updates. *Computer Methods in Applied Mechanics and Engineering* 1999; **171**:419–444.
26. Radovitzky R and Ortiz M. Error estimation and adaptative meshing in strongly nonlinear dynamics problems. *Computer Methods in Applied Mechanics and Engineering* 1999; **172**:203–240.
27. Simo JC and Taylor RL. Quasi-incompressible finite elasticity in principal stretches continuum basis and numerical algorithms. *Computer Methods in Applied Mechanics and Engineering* 1991; **85**:273–310.
28. Antman SA. *Non Linear Problems of Elasticity*. Springer-Verlag, 1995.
29. Fraijs de Veubeke BM. *Diffusion des inconnues hyperstatiques dans les voilures à longerons couplés*, volume 24 of *Bulletins du Service Technique de L'Aéronautique*. Imprimerie Marcel Hayez, Bruxelles, Belgium, 1951.
30. Hu HC. On some variational methods on the theory of elasticity and theory of plasticity. *Scientia Sinica* 1955; **4**:33–54.
31. Washizu K. On the variational principles of elasticity and plasticity. Technical Report 25-18, Aeroelastic ans Structures Research Laboratory, Massachusetts Institute of Technology, Cambridge, USA, 1955.
32. Felipa CA. On the original publication of the general canonical functional of linear elasticity. *Journal of Applied Mechanics* 2000; **67**(1):217–219.
33. Crisfield MA. *Non-linear finite element analysis of solids and structures*, volume 1. John Wiley and Sons, 2001.
34. Gonzalez O and Simo JC. On the stability of sympletic and energy-momentum algorithms for non-linear Hamiltonian systems with symmetry. *Computer Methods in Applied Mechanics and Engineering* 1996; **134**:197–222.

35. Simo JC. Algorithms for static dynamic multiplicative plasticity that preserve the classical return mapping schemes of the infinitesimal theory. *Computer Methods in Applied Mechanics and Engineering* 1992; **99**:61–112.

36. Hughes TJR. Stability, convergence and growth and decay of energy of the average acceleration method in nonlinear structural dynamics. *Computers & Structures* 1976; **6**:313–324.

37. Noels L, Stainier L, and Ponthot J-P. Simulation of crashworthiness problems with improved contact algorithms for implicit time integration. *International Journal of Impact Engineering.* Accepted for publication.

List of Figures

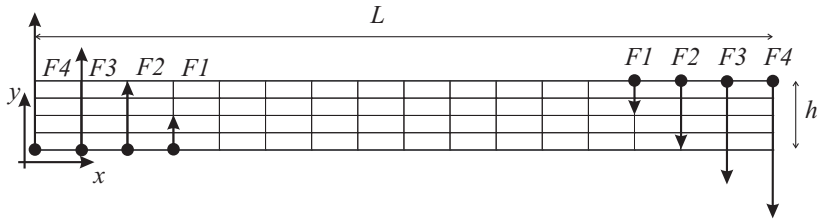

Figure 1. Geometry and loading of the tumbling beam.

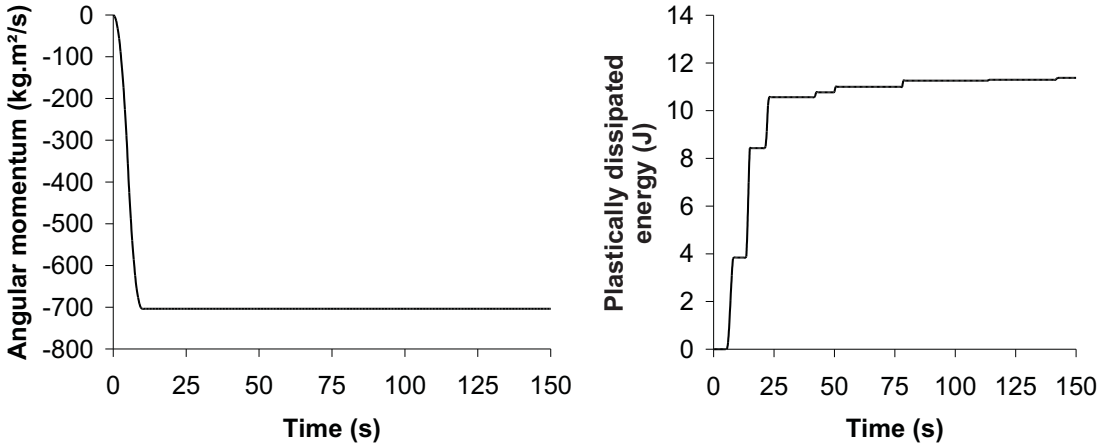

(a) Angular momentum

(b) Plastically dissipated energy

Figure 2. Time evolution for the tumbling beam.

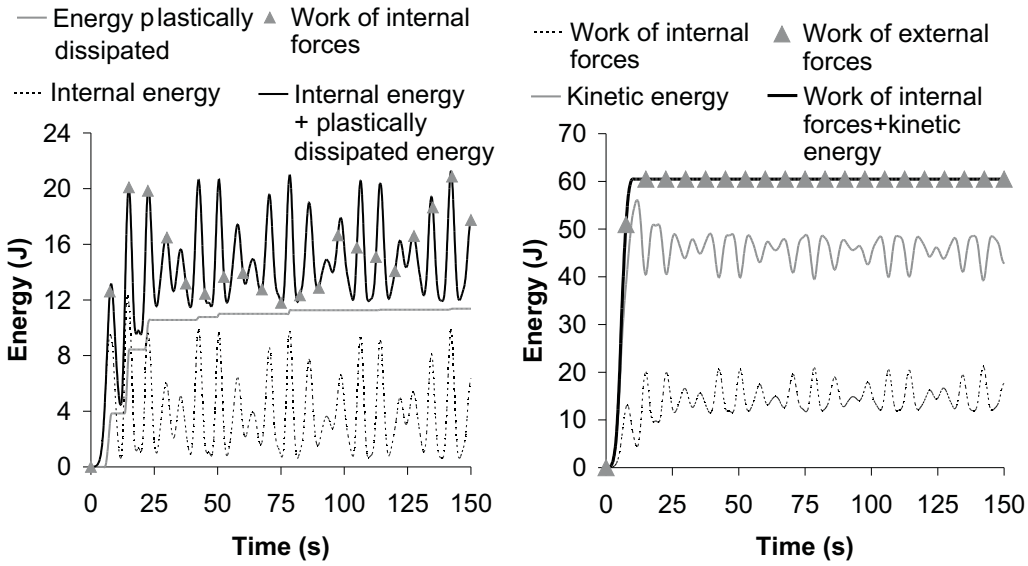

(a) Internal energy

(b) Total energy

Figure 3. Energy balance for the tumbling beam.

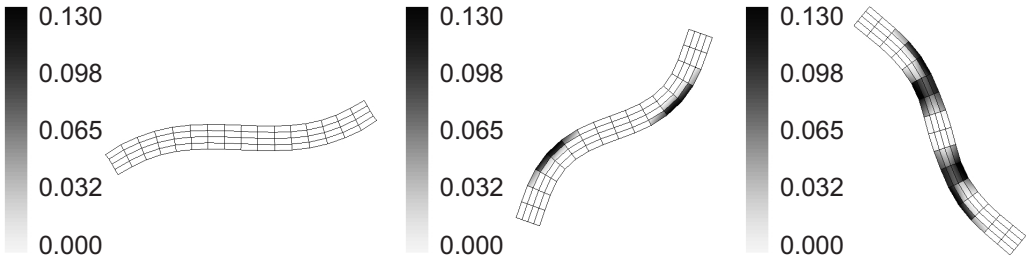

(a) $t = 5s$ (b) $t = 10s$ (c) $t = 150s$

Figure 4. Equivalent plastic strain.

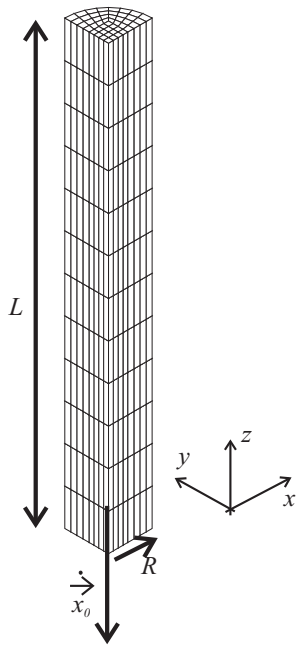

Figure 5. Initial geometry of the Taylor's bar.

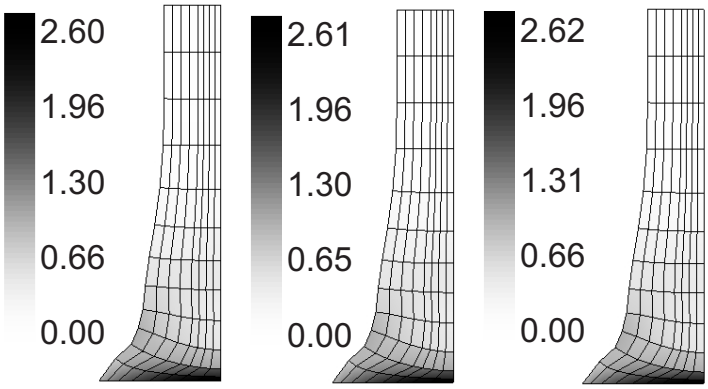

(a) $\Delta t = 0.025\mu s$ (b) $\Delta t = 0.1\mu s$ (c) $\Delta t = 0.4\mu s$

Figure 6. Equivalent plastic strain for the Taylor's bar with the EMCA scheme.

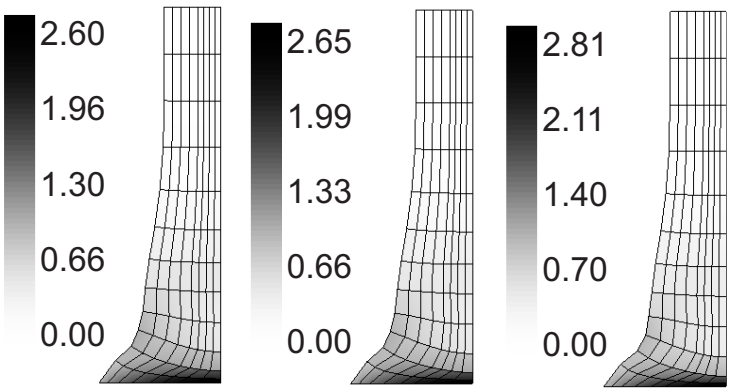

(a) $\Delta t = 0.025\mu s$ (b) $\Delta t = 0.1\mu s$ (c) $\Delta t = 0.4\mu s$

Figure 7. Equivalent plastic strain for the Taylor's bar with the Newmark scheme.

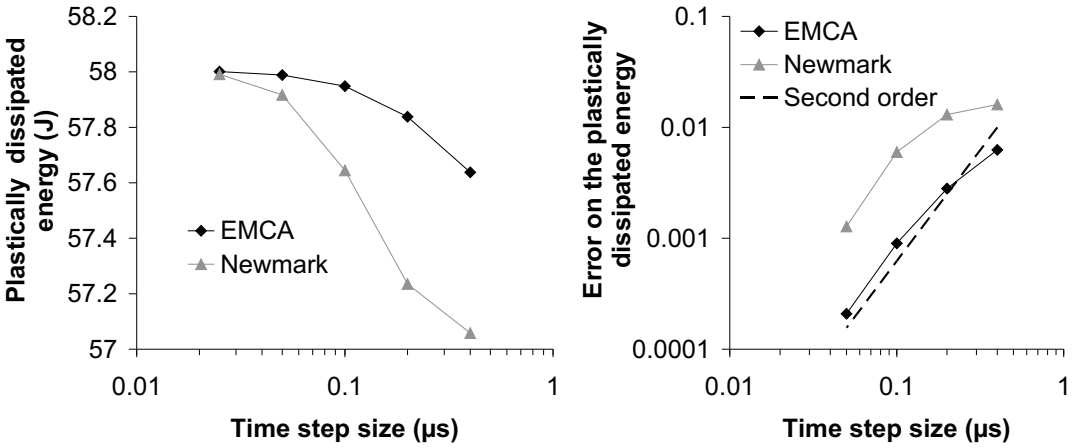

(a) Final energy

(b) Error on final energy

Figure 8. Plastically dissipated energy for the Taylor's bar (logarithmic scales).

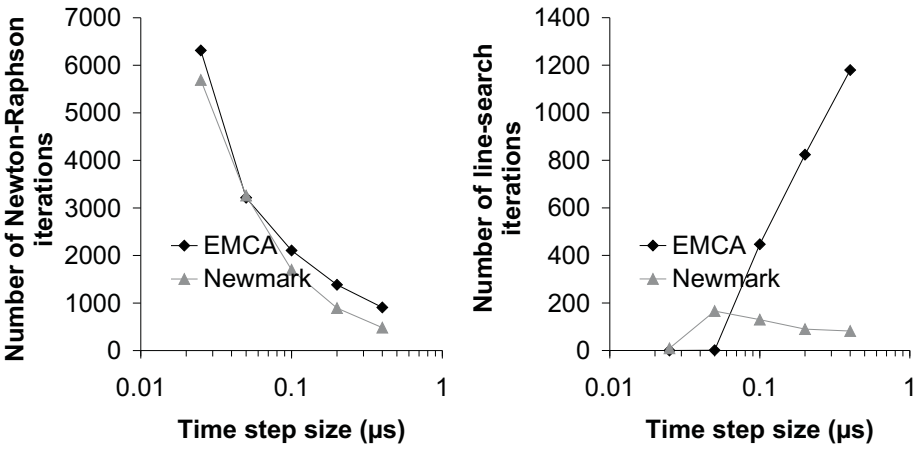

(a) Newton-Raphson iterations (b) Line-search iterations

Figure 9. Number of iterations for the Taylor's bar.

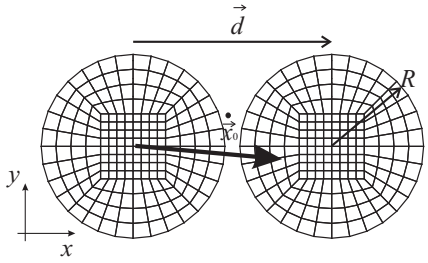

Figure 10. Geometry and initial velocity of the two cylinders.

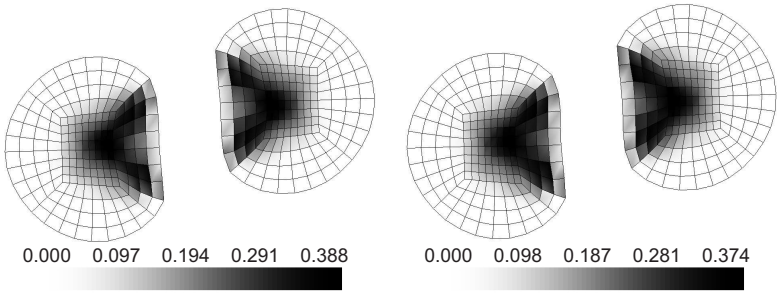

(a) EMCA (b) Newmark

Figure 11. Equivalent plastic strain for the two cylinders with $\Delta t = 2.5ms$.

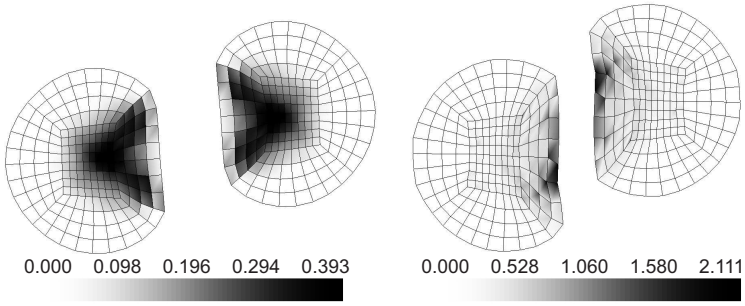

(a) EMCA (b) Newmark

Figure 12. Equivalent plastic strain for the two cylinders with $\Delta t = 20ms$.

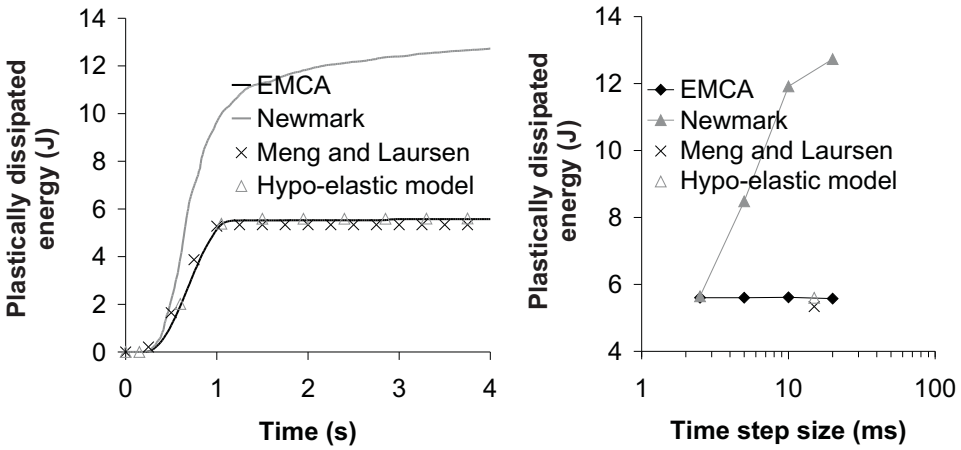

(a) Time evolution for $\Delta t = 20ms$ (b) Final results

Figure 13. Plastically dissipated energy for the two cylinders.

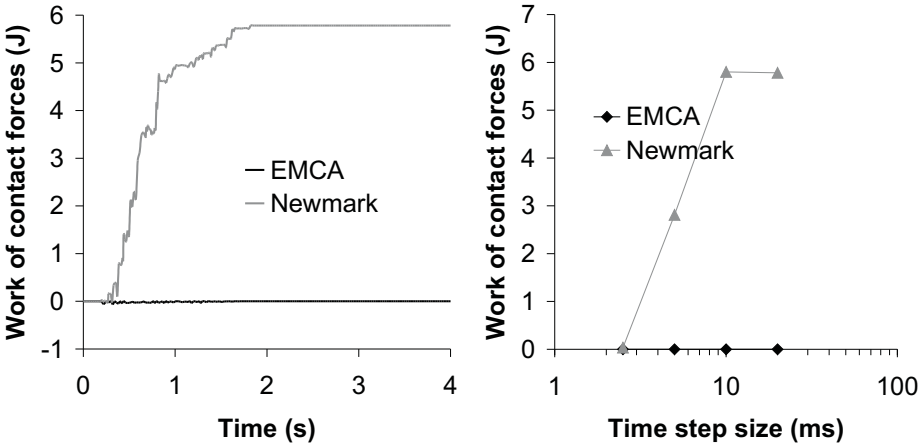

(a) Time evolution for $\Delta t = 20ms$ (b) Final results

Figure 14. Work done by contact forces for the cylinders problem.

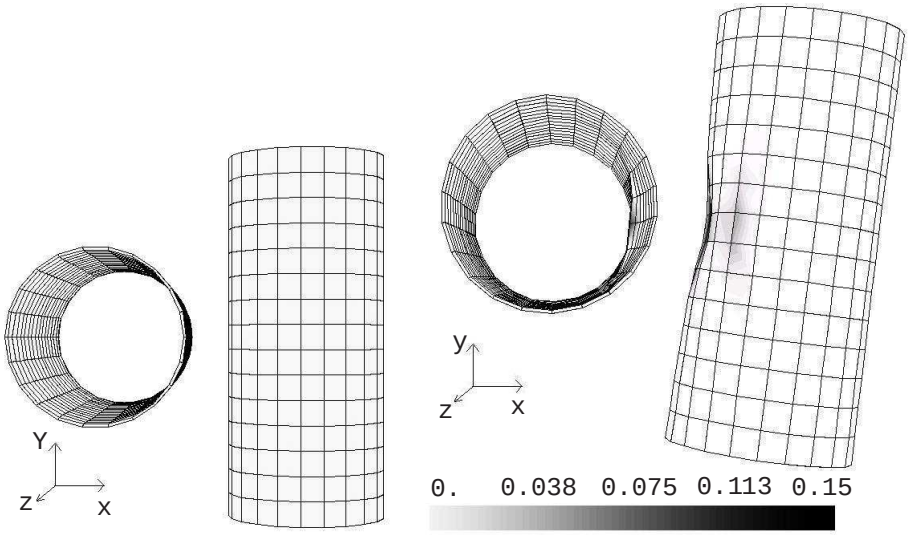

(a) $t = 0ms$ (b) $t = 10ms$

Figure 15. Geometry and equivalent plastic strain for the two hollow cylinders.

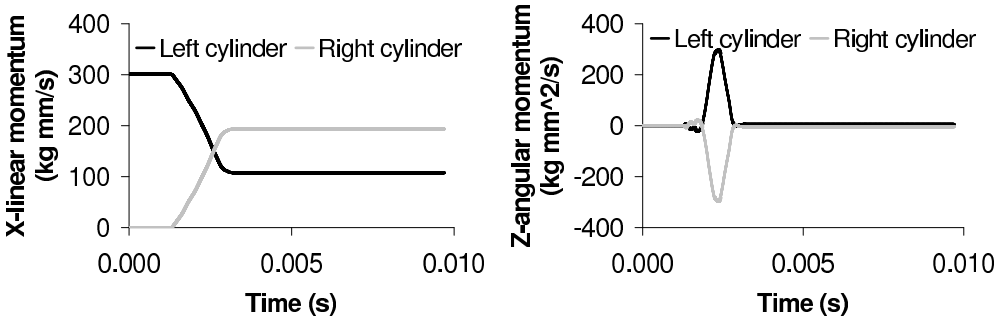

(a) Linear momentum (b) Angular momentum

Figure 16. Time evolution of the momenta for the hollow cylinders.

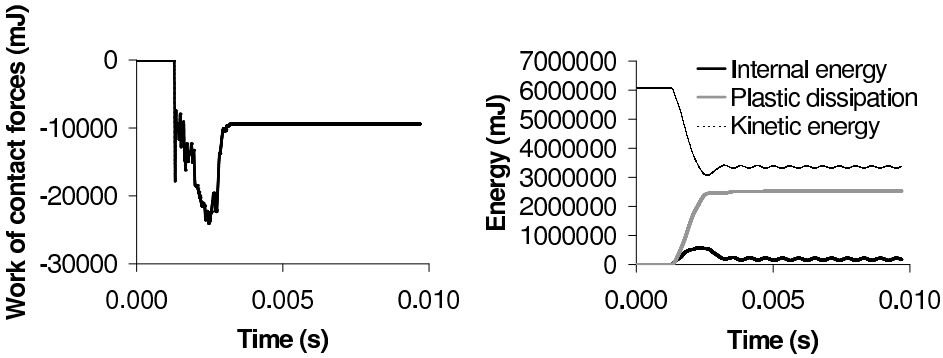

(a) Work of contact forces (b) Energy

Figure 17. Time evolution of the energies of the two hollow cylinders.

List of Tables

Table I. Properties of the tumbling beam.

Properties	Values
Length	$L = 16m$
Height	$h = 1m$
Initial density	$\rho_0 = 10kgm^{-3}$
Bulk modulus	$K_0 = 500Nm^{-2}$
Shear modulus	$G_0 = 40Nm^{-2}$
Initial yield stress	$\Sigma_0 = 15Nm^{-2}$

Table II. Properties of the Taylor's bar.

Properties	Values
Radius	$R = 0.0032m$
Length	$L = 0.0324m$
Initial velocity	$\dot{\vec{x}}_0 = (0; 0; -227ms^{-1})$
Initial density	$\rho_0 = 8930kgm^{-3}$
Bulk modulus	$K_0 = 130000Nmm^{-2}$
Shear modulus	$G_0 = 433333Nmm^{-2}$
Initial yield stress	$\Sigma_0 = 400Nmm^{-2}$
Linear hardening	$h = 100Nmm^{-2}$

Table III. Final results for the Taylor's bar.

Scheme	Radius	Length	$\varepsilon^{\mathrm{pl}}$
EMCA, $\Delta t = 0.05\mu s$	$0.006774m$	$0.02140m$	2.61
EMCA, $\Delta t = 0.025\mu s$	$0.006775m$	$0.02140m$	2.62
EMCA, $\Delta t = 0.1\mu s$	$0.006777m$	$0.02140m$	2.60
EMCA, $\Delta t = 0.2\mu s$	$0.006783m$	$0.02140m$	2.61
EMCA, $\Delta t = 0.4\mu s$	$0.006813m$	$0.02141m$	2.61
Newmark, $\Delta t = 0.025\mu s$	$0.006774m$	$0.02140m$	2.61
Newmark, $\Delta t = 0.05\mu s$	$0.006778m$	$0.02140m$	2.62
Newmark, $\Delta t = 0.1\mu s$	$0.006798m$	$0.02142m$	2.65
Newmark, $\Delta t = 0.2\mu s$	$0.006842m$	$0.02145m$	2.74
Newmark, $\Delta t = 0.4\mu s$	$0.006874m$	$0.02146m$	2.81
Simo [35], $\Delta t = 0.5\mu s$	$0.00697m$	-	-
Meng and Laursen [9], $\Delta t = 1\mu s$	0.006775	$0.02164m$	2.62
Hypo-elastic [12], $\Delta t = 0.5\mu s$	$0.006553m$	$0.02158m$	2.37

Table IV. Properties of the two cylinders.

Properties	Values
Radius	$R = 1m$
Distance between the two gravity centers	$\vec{d} = (2.18m; 0m)$
Initial velocity of left cylinder	$\dot{\vec{x}}_0 = (1ms^{-1}; -0.1ms^{-1})$
Initial density	$\rho_0 = 8.93kgm^{-3}$
Bulk modulus	$K_0 = 130Nm^{-2}$
Shear modulus	$G_0 = 43.3Nm^{-2}$
Initial yield stress	$\Sigma_0 = 10Nm^{-2}$
Normal penalty of contact	$k_N = 10^4$

Table V. Properties of the two hollow cylinders.

Properties	Values
Mean radius	$R = 98.5mm$
Thickness	$e = 3mm$
Distance between the two gravity centers	$\vec{d} = (250mm; 0mm; 0mm)$
Initial velocity of left cylinder	$\dot{\vec{x}}_0 = (40ms^{-1}; 4ms^{-1}; 0ms^{-1})$
Initial density	$\rho_0 = 8930kgm^{-3}$
Bulk modulus	$K_0 = 130000Nmm^{-2}$
Shear modulus	$G_0 = 433333Nmm^{-2}$
Initial yield stress	$\Sigma_0 = 400Nmm^{-2}$
Linear hardening	$h = 100Nmm^{-2}$
Normal penalty of contact	$k_N = 10^5$
Tangential penalty of contact	$k_T = 10^3$
Coulomb coefficient	$\mu_c = 0.1$